Natural Hazards (2026) 122:255
https://doi.org/10.1007/s11069-025-07767-2

ORIGINAL PAPER

Multi-risk assessment in the NW coast of the Island of Malta (central Mediterranean Sea)

Nabanita Sarkar[1,2] · **Angela Rizzo**[3,4] · **Vittoria Vandelli**[5] · **Mauro Soldati**[5]

Received: 31 July 2025 / Accepted: 24 November 2025
© The Author(s), under exclusive licence to Springer Nature B.V. 2026

Abstract
Ongoing climate change is leading to increased vulnerability of coastal communities and anthropogenic activities, exposing them to multiple hazards. Coastal areas are increasingly prone to be affected by weather- and climate-related processes: erosion, flooding, slope instability, and, on a longer-term, permanent inundation due to sea level rise. In this context, studies aiming at defining potential multi-risk scenarios serve as an essential tool for recognizing the most effective coastal management strategies and adaptation measures. In this research, a multi-risk framework was applied to assess and map the level of coastal risk along the north-west coast of the Island of Malta, central Mediterranean Sea. To this aim, the exposure, vulnerability and susceptibility levels to different physical processes (temporary and permanent inundation, shoreline erosion and rock fall) were estimated using an index-based approach. Then, the multi-risk assessment for the end-century period (2100) was calculated and mapped by exploiting GIS tools. The results highlight that the bays are the most critical zones in the investigated coastal sector. Under the worst-case conditions in 2100, medium-risk zones account for approximately 23% of the investigated area, while 6% falls under high-risk.

Keywords Climate change · Coastal risk · Sea level rise · Storm surge · Rock fall · Erosion · Malta

1 Introduction

Since the late 20th century, climate change has increasingly affected both natural environments and human systems worldwide, as evidenced by accelerating warming trends and the growing frequency of climate-related hazards. Climate change, and its related impacts, became a formally recognized global environmental issue after the publication of the first the Intergovernmental Panel on Climate Change Assessment Report (IPCC 1990) and the signing of the UNFCCC in 1992.

As highlighted by the most updated data, weather patterns are changing, causing extreme events (i.e., storm surges, torrential rain, heat waves, fires) to occur more frequently in dif-

Extended author information available on the last page of the article

Published online: 27 February 2026

ferent parts of the world (IPCC 2023). Coastal areas are being exposed to multiple climate change impacts such as increased flood frequency, saltwater intrusion, erosion, and, on a longer term, sea-level rise (Nicholls and Hoozemans 1996; IPCC et al. 2007; Nicholls and Cazenave 2010; Torresan et al. 2012; IPCC 2013; Lyra et al. 2024; Schuerch et al. 2025).

In the First Assessment Report on Climate and Environmental Change in the Mediterranean, it is highlighted that the Mediterranean region is warming 20% faster than the global average. In the Mediterranean basin, the observed rates of climate change surpass the worldwide trends for most of the accounted variables (Cramer et al. 2018). In the past years, a temperature increase has been observed in the surface of the upper layer of the Mediterranean Sea by approximately 0.5° (Todaro et al. 2022). Over the last two decades, sea levels have risen at a rate of approximately 3 cm per decade in the Mediterranean region (Cramer et al. 2018). Considering the fact that the effects of climate change are expected to be stronger there than in other areas of the world, the Mediterranean can be considered a "hotspot" of climate change (Giorgi 2006; Giorgi and Lionello 2008; Lionello and Scarascia 2018; Sarkar et al. 2022; Vandelli et al. 2023; Rossi et al. 2025a).

A wide number of studies have assessed the vulnerability of the Mediterranean in light of direct and indirect climate-related impacts along the coast (Khouakhi et al. 2013; Frihy and El-Sayed 2013; Tarragoni et al. 2014; Aucelli et al. 2018; Rizzo et al. 2022). Many of these studies have focused on potential permanent inundation due to sea level rise (SLR) and related impacts on coastal landscapes and local economies. In this context, several works have provided assessments based on future sea level projections coupled with tectonic and glacio- hydro-isostatic contributions to refine estimate of relative sea-level change (Lambeck et al. 2011; Pappone et al. 2012; Antonioli et al. 2017; Marsico et al. 2017; Perini et al. 2017; Anzidei et al. 2018; Scardino 2020). Other works have further examined the local contribution of vertical land movements by quantifying displacement rates from satellite data (Anzidei et al. 2017, 2021; Aucelli et al. 2017; Di Paola et al. 2021; Scardino et al. 2022) and Global Navigation Satellite System (GNSS) stations (Anzidei et al. 2020). Collectively, these studies hint towards the risk of anthropic and natural assets, as well as cultural heritage sites, being impacted by coastal processes associated with sea level rise and related impacts.

As mentioned above, rising sea level is also expected to exacerbate coastal erosion, particularly along sandy shorelines and mobile coastal systems. Sedimentary coasts, which include sandy beaches, dune systems and wetlands, constitute 46% of the Mediterranean coast (Brochier and Ramieri 2001). Several studies have been carried out to assess coastal vulnerability to erosion (Jiménez et al. 2017; Monioudi et al. 2017; Enríquez et al. 2019), indicating that the Mediterranean shores are prone to increased retreat (Brochier and Ramieri 2001; Velegrakis et al. 2023). Such process affects the natural ecosystems, anthropic structures, and local economies, especially the tourism sector, which is often the main economic activity in Mediterranean coastal areas and islands (Mejjad et al. 2022). In addition, numerous studies related to storm surge impact along the Mediterranean coasts indicate that this region is particularly prone to storm- induced temporary flooding (Amores et al. 2020; Androulidakis et al. 2023; Scardino et al. 2022; Abouelnasr and Elselmy 2024).

Moreover, increased rainfall variability observed over the last 50 years in the Mediterranean—where precipitation is already subject to pronounced inter-annual fluctuations (Longobardi and Boulariah 2022; Menna et al. 2022)—reflects a change in the magnitude and frequency of precipitation events in this region.

Therefore, based on the above assumptions, the Mediterranean coastal areas are increasingly considered exposed to significant risks from a range of multiple climate-related processes (Gallina et al. 2016, 2020; Prampolini et al. 2020). Coastal risk is usually evaluated by means of index-based approaches and considering the spatial combination of (i) physical susceptibility to accounted processes, (ii) exposure of natural and anthropic elements, and (iii) vulnerability of exposed assets or communities (Rizzo et al. 2020, 2022; Pantusa et al. 2022; Manno et al. 2023; Batzakis et al. 2024). The index-based approach was exploited at the European scale in the framework of the EUROSION Project in 2004 to assess coastal exposure to marine-related processes, including flooding and erosion (Bruno et al. 2020). Afterwards, several studies have been conducted in the Mediterranean countries by exploiting this approach for coastal risk and vulnerability analysis, as highlighted in Rizzo et al. (2025). Stakeholders in both public and private organizations are seeking spatially-explicit information regarding coastal risks to climate change at the local scale. Furthermore, there is a growing need for identifying the most vulnerable areas, as well as mapping the potential impacts on natural assets and critical infrastructures, and supporting the identification of efficient adaptation measures (Christodoulou et al. 2019; De Vivo et al. 2022). In this context, this paper provides a first attempt to assess multiple coastal risks along the northwest coast of the island of Malta, in the central Mediterranean Sea. Due to its geographical, geological and structural characteristics, the area is particularly prone to be affected by multiple climate-related processes (Main et al. 2018). Nevertheless, to date, there are no studies in the literature that comprehensively address coastal risk in this region. Therefore, this article aims to provide a recognition of the ongoing and expected processes that could affect the investigated coastal stretch in the near future. Based on the current distribution of the exposed elements and taking into account two alternative climate scenarios, the multi-risk assessment for the year 2100 is provided in the form of quantitative indicators and qualitative spatial mapping.

2 Study area

Three main islands—Malta, Comino, and Gozo—together with a few smaller uninhabited islets constitute the Maltese Islands (Schembri 2019; Rossi et al. 2024), which host remarkable environmental and cultural values (Coratza et al. 2016; Possenelli et al. 2024). They are located in the central Mediterranean Sea, approximately 90 km south of Sicily and 270 km north-east of Tunisia (Fig. 1). Long-term tectonic and geomorphological processes, also due to sea level changes related to climatic variations, have shaped the Maltese landscapes and landforms through time (Micallef et al. 2013; Foglini et al. 2016; Soldati et al. 2018; Galea 2019; Gauci and Schembri 2019; Prampolini et al. 2019; Rossi et al. 2025b).

The Maltese Islands currently experience a Mediterranean temperate climate, with a mean annual temperature of ca. 19.5 °C and an average annual precipitation of ca. 550 mm (reference period 1991–2020; NSO 2022; Mifsud Scicluna and Galdies 2025). However, rainfall is characterised by a high interannual variability with annual total ranging from a minimum of 274.2 mm (1961) to a maximum of 900.6 mm (2003) during the period 1952–2020 (NSO 2022). Although the overall rainfall regime has become drier, short-duration extreme rainfall events still occur. The annual maximum daily rainfall has reached values exceeding 100 mm in several years (reference period 1980–2005; Russo et al. 2022). More-

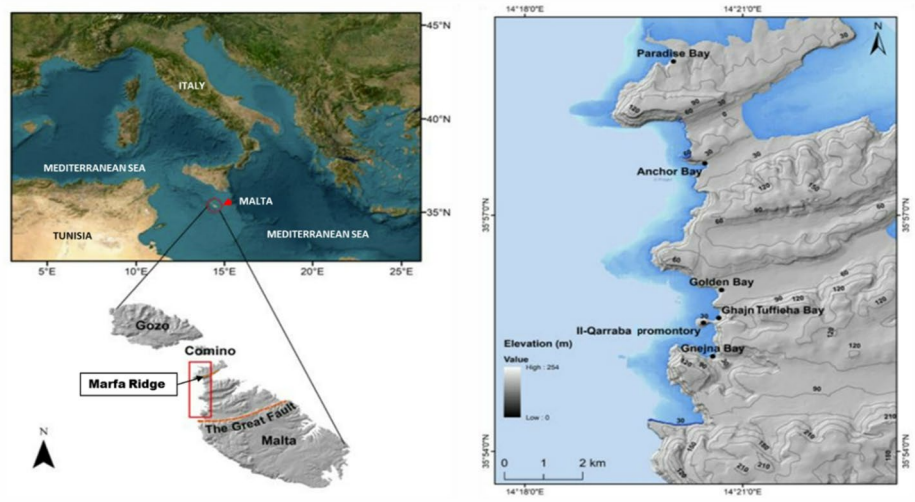

Fig. 1 Geographic setting of the study area and location of the investigated sites along the north–west coast of Malta. The satellite image is derived from ArcGIS Online World Imagery © Esri and its data providers. Modified after Sarkar et al. (2024)

over, the frequency of heavy rainfall events and storms exhibit an upward trend, confirming that the Maltese Islands are increasingly prone to weather extremes (Mayes 2001; NSO 2022; Russo et al. 2022).

The study area extends along the north-west coast of the island of Malta, bounded by the Marfa Ridge to the north and the Great Fault to the south (Devoto et al. 2012; Soldati et al. 2019).

In particular, the study investigates the coastal stretch from Paradise Bay to Gnejna Bay, including six major embayments (Fig. 1). This area is of high geomorphological, environmental and socio-economic importance (Prampolini et al. 2017; Soldati et al. 2019). It hosts several pocket beaches (Zammit Pace et al. 2019), a natural park encompassing rich geoheritage sites (Coratza et al. 2011; Cappadonia et al. 2018; Selmi et al. 2019), and numerous recreational facilities, including an amusement park. Furthermore, this coastal zone hosts Special Protection Areas included in the Natura 2000 network (Spiteri and Stevens 2019). In this context, the investigated area concentrates a significant portion of natural assets, tourist activities and infrastructures, which in turn have increased exposure and vulnerability to climate-related hazards.

From a geological viewpoint, the investigated stretch of coast comprises a stratigraphic sequence ranging from the age of late Oligocene to the late Miocene. Outcropping rocks belong to a marine sedimentary succession consisting of five lithostratigraphic units including limestones, clays and marls covered by thin superficial deposits (Pedley et al. 1978; Scerri 2019). The stratigraphic succession, from the oldest to the youngest, includes the Lower Coralline Limestone, Globigerina Limestone, Blue Clay, Greensand, and Upper Coralline Limestone formations (cf. Fig. 2; Baldassini and Di Stefano 2017). The Upper Coralline Limestone forms plateaus affected by a dense network of joints and characterized by steep escarpments, which are continuously shaped by gravity-induced and degradation processes. The underlying Blue Clay forms gentle slopes progressing towards the sea and

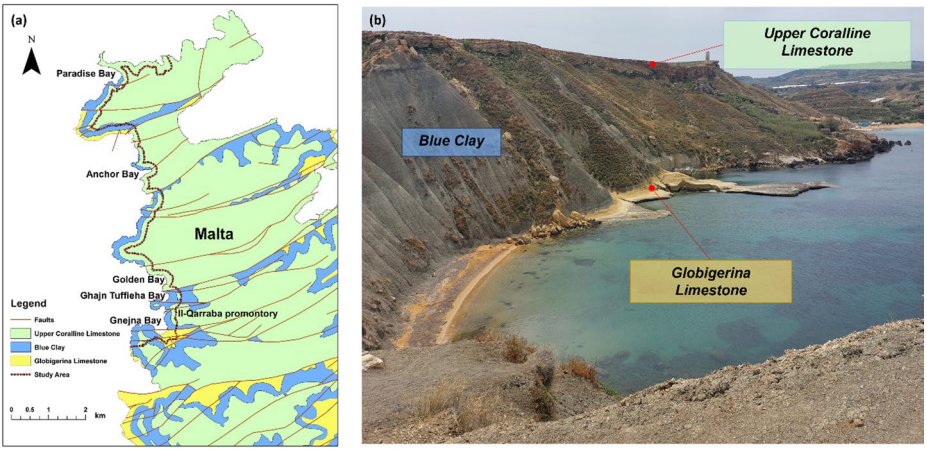

Fig. 2 Geological setting of the study area showing the main lithostratigraphic units. Greensand is not depicted due to its limited outcrops, which make it unmappable at this scale. **a** Geological sketch map **b** Qarraba Bay site. The red dashed line identifies the inland boundary of the study area

often hosting active or abandoned terraced cultivation fields. The Globigerina Limestone only outcrops in the southern sector, near Gnejna Bay, and in the northern sector, near the Marfa Ridge. There, it is exposed at the sea level and gives rise to shore platforms and cliffs.

The marked geomechanical contrast between the brittle Upper Coralline Limestone and the underlying ductile Blue Clay favours the development of extensive lateral spreading. In association with the latter, rock falls often affect the Upper Coralline Limestone. Detached limestone boulders accumulate on the clayey slopes below and are displaced by earth flows/slides in the form of block slides (cf. Mantovani et al. 2013; Mantovani et al. 2016; Devoto et al. 2020). Geomorphological investigations suggest that marine erosion can enhance the occurrence of mass movements, whereas accumulations of rock blocks at sea level can mitigate the impact of wave erosion and coastline retreat (Devoto et al. 2012).

The investigated stretch of coast presents various coastal geomorphotypes (Fig. 3) and includes both natural and anthropogenic features of high geomorphological and socio-economic relevance. All the embayments, except for Anchor Bay, host pocket sandy beaches, being Golden Bay beach one of the largest of the Island. These pocket beaches constitute key landscape features as well as ecological, and economic resources for an island largely characterized by rocky coasts. Their potential degradation or loss, e.g., due to marine erosion, can cause significant environmental damage and economic repercussions (Micallef et al. 2018).

The investigated area is extensively used for tourism and recreational purposes, including facilities and infrastructures some of which are located in proximity to unstable cliffs susceptible to rock falls.

Traditional maritime structures are also present, such as the boathouses at Gnejna Bay, which are located at or slightly above sea level, making them potentially exposed to storm surges and coastal erosion.

Overall, the study area hosts specific sites that include numerous elements potentially exposed to risk as a consequence of various coastal hazards such as erosion, slope instability, flooding, and improper planning of anthropogenic interventions. The assets also include

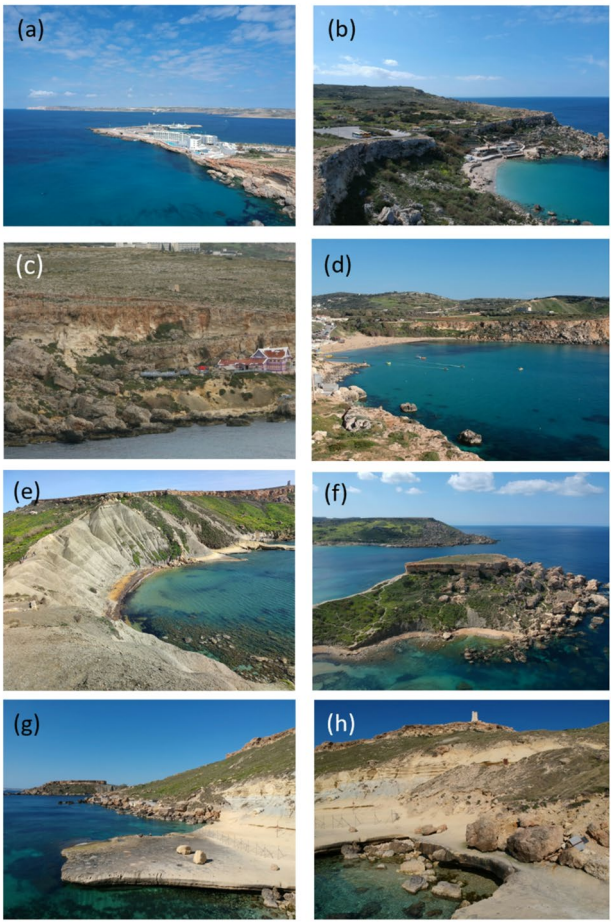

Fig. 3 Main geomorphological features and processes of the study area: **a** built-up coast at Cirkewwa harbour and surroundings; **b** pocket beach at Paradise Bay; **c** rock falls and block slides at Anchor Bay; **d** cliff and pocket beach at Golden Bay; **e** gully erosion affecting clayey terrain at Qarraba Bay; **f** rock spreading and block sliding at Il-Qarraba promontory; **g** sloping coast and pocket beach and **h** shore platform at Gnejna Bay

remarkable ecological areas, coastal footpaths, trails that connect the cliffs to the beach, cultural heritage, and local infrastructure.

3 Materials and methods

3.1 Procedure for risk assessment

In the context of climate change, since 2013, the IPCC has adopted the definition of "risk" as an outcome of the interaction between climate-related hazards, exposure, and vulner-

ability of the anthropic or ecological systems potentially impacted by a particular physical process.

Therefore, with respect to this definition, which was firstly proposed by the disaster risk reduction community, the evaluation of exposed elements (E) and related vulnerability (V) needs to be connected with hazard (H) informative layer. The latter is connected to the temporal occurrence (return period) and spatial pattern distribution (potentially affected area) of the potentially hazardous physical event. Nevertheless, for long-term processes such as SLR, assessing frequency is challenging. Instead, assessing the susceptibility of the territory to be affected by SLR is deemed more beneficial.

By combining exposure, vulnerability, and hazard/susceptibility into a multiplicative risk formula, the spatial zonation of the area under investigation can be obtained.

The methodological steps proposed to assess the coastal multi-risk along the north-west coast of Malta are elucidated in the following sub-sections and schematically summarized in Fig. 4.

3.2 Phase 1: Coastal exposure (E) and vulnerability (V) assessment

According to the index-based approach, coastal exposure and vulnerability are evaluated taking into account tailored indicators, whose spatial overlay provides an estimate of their semi-quantitative value, classified in five classes ranging from "very low" to "very high". For this kind of analysis specific GIS tools were used to identify coastal assets and to map the exposure and vulnerability levels of the investigated zones, as illustrated in Sub-Sect. 3.2.1–3.2.3.

3.2.1 Definition of the landward limit of the coastal investigated area

The limits of the study area were identified by considering the RICE area (Radius of Influence of Coastal Erosion and Flooding) proposed in the framework of the EUROSION project to identify coastal assets exposed to potential impacts of marine-related processes (Salman et al. 2004). The RICE limit, normally set at a distance of 500 m inland or reaching a maximum of 5 m a.s.l., was in this case extended up to 100 m from the cliff, thus including the edge of the cliffs formed in the Upper Coralline Limestone, which are particularly

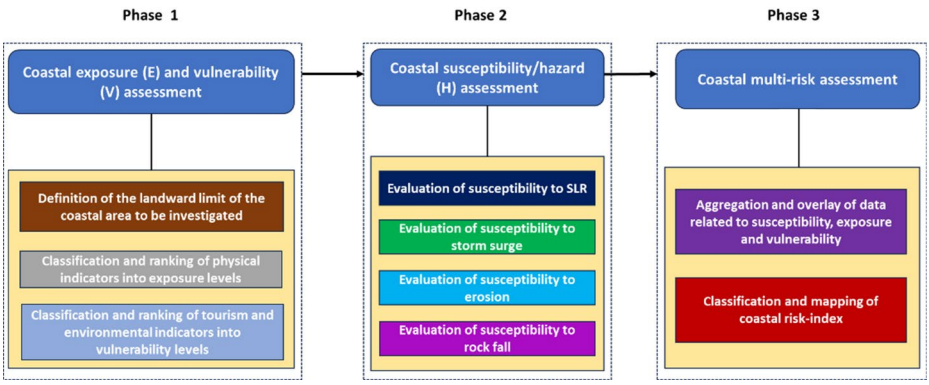

Fig. 4 Framework for coastal multi-risk assessment adopted in this study

prone to rock-fall process. The landward limit shown in Fig. 2 was simplified by using a red coloured line to better represent the coastal sector under investigation.

3.2.2 Classification and ranking of physical indicators into exposure classes

In this stage, data for physical indicators defining anthropic and natural assets like land use, transport network and utilities potentially exposed to coastal hazards were collected and ranked following the approach proposed in Rizzo et al. (2020). The creation of a GIS layer for each indicator aided in the identification of polygons that correspond to the spatial unit to which a related exposure class is assigned. The exposure classes range from "very low exposure" (Class 1) to "very high exposure" (Class 5). The layers were overlaid to calculate the exposure values associated with each cell in the raster format. In Table 1, a detailed view of the exposure classes assigned to each category is provided.

Land use data were gathered from CORINE Land Cover (2018) containing the spatial classification of different land cover and land use categories. CORINE data were supplemented with more detailed information so as to include boat houses, beaches, dunes derived from the interpretation of recent satellite images of the investigated area and corroborated

Table 1 Physical indicators and expert-based exposure classes assigned to each category of assets. Exposure classes range from "very low exposure" (Class 1) to "very high exposure" (Class 5)

	Very low	Low	Medium	High	Very high
Physical indicators	Class 1	Class 2	Class 3	Class 4	Class 5
Land Cover/ Land Use	Bare rock, heath, sparsely vegetated area	Farmland, Agricultural area, Land principally occupied by agriculture, with significant areas of natural vegetation, Sclerophyllous vegetation	Industrial area, park, grasslands, residential area, discontinuous urban fabric	Beaches, dunes	Historical and archaeological sites, Entertainment (commerce, finance, business, recreational, leisure, and sport)
Transport	Absent or degraded transport network	Footway, path, track, step, pedestrian road, cycleway	Tertiary, service, residential, trunk roads	Secondary roads	Primary road
Utilities	Absence of utilities	Local and small utilities	Street lighting	11 kV overhead line	Feeder pillar

by field surveys. An exposure class was assigned to each land use category on the basis of expert-based judgments. In detail, the highest exposure class was assigned to zones occupied by entertainment spots, historical buildings, and archaeological sites, while bare grounds and sparsely vegetated areas were assigned to the lowest exposure class.

Open Street Map data downloaded from "Geofabrik" (2024) were used to obtain the local transport network. To account for a proper area of significance, a buffer distance of 5, 10, 15 and 20 m was built to each of the above-mentioned transport network polylines, respectively, with the exception of "absent or degraded transport network".

The spatial data regarding utilities were gathered from the Malta Inspire Geoportal. In this case, a buffer distance of 5, 10, 15 and 20 m was built for local/small utilities, street lighting, 11 Kv overhead line and feeder pillars, respectively, with the exception of "absence of utilities".

3.2.3 Classification and ranking of tourism and environmental indicators into vulnerability classes

The vulnerability analysis was performed based on the characterization of the six investigated bays by direct and indirect evaluation of the tourism and environmental setting, taking into account the number of visitors attending these sites and the presence of natural protected areas.

In detail, the tourism vulnerability is here defined as tourism pressure in the investigated zones and is evaluated in terms of number of pictures and number of reviews posted on Google. The number of natural protected sites prevailing in these areas gave an indication of the environmental pressure. Former data were retrieved from Google Maps, user-generated contents and the latter from Open Street Map.

Specifically, the total number of pictures uploaded, the total number of reviews posted for each site, and the natural protected areas were selected as indicators for the overall vulnerability analysis. These data were normalised, combined into a single vulnerability score and then classified based on the geometric mean of the values attributed to each indicator. Five classes from "very low vulnerability" (Class 1) to "very high vulnerability" (Class 5) were defined by means of an equal interval classification method.

3.3 Phase 2: Coastal susceptibility/hazard (H) assessment

In order to assess the expected coastal multi-risk scenarios, the susceptibility to different marine- and climate-related processes (i.e., permanent and temporary inundation, erosion, rock fall) was evaluated. Each susceptibility analysis allowed the zonation of the investigated areas in five susceptibility classes, ranging from "very low susceptibility" (Class S1) to "very high susceptibility" (Class S5).

Specific GIS-based raster analysis tools were used for the susceptibility assessment and mapping. High-resolution topographic data consisting of LiDAR-derived Digital Terrain Model with 1 m resolution (ERDF 156 Data 2013) were used for the assessment of susceptibility to SLR, storm surge and rock fall. For assessing the susceptibility to erosion in the last 20 years, orthophotos of the investigated zones were analysed.

3.3.1 Evaluation of susceptibility to SLR

For the analysis of susceptibility to SLR, based on the topographic setting, the study area was classified into five classes, ranging from "very low or almost zero susceptibility" (Class S1), including areas with a topographic height in the range of >5 m a.s.l., to "very high susceptibility" (Class S5), including areas with topographic height≤0 m and therefore considered prone to permanent inundation due to SLR (cf. Rizzo et al. 2022 and Vandelli et al. 2023 for the area of Gozo; Table 2).

The study made use of the local projected sea level for the long-term period referring to the year 2100 under two Shared Socioeconomic Pathways (SSP), namely SSP1-2.6 and SSP5-8.5, corresponding respectively to the best- and worst-case scenario for future climate conditions. The NASA Sea level projection tool (available at https://sealevel.nasa.gov/ipcc-ar6-sea-level-projection-tool) was used for downloading the local sea level projections referred to the baseline period 1995–2014 (IPCC 2023). Consequently, the local sea level values used in the study are 0.47 m (likely range 0.26–0.71 m) for the best-case scenario (SSP1-2.6) and 0.80 m (likely range 0.57–1.11 m) for the worst-case scenario (SSP5-8.5).

3.3.2 Evaluation of susceptibility to storm-surge

To assess the susceptibility to temporary increase in sea level, the study took advantage of the Total Water Level (TWL) indicator available from the Copernicus platform Climate Data Store (CDS). TWL indicator defines the water level including tide, surge level and taking future sea level rise into account, for different return periods (2, 5, 10, 25, 50 and 100 years). The vertical reference level is mean sea level (MSL) over the 1986–2005 reference period and with a horizontal resolution of 0.1° (11.1 km) along the coastal sectors. In this study, the long-term period (2071–2100) was considered, corresponding to the end-of-century time frame adopted for sea level projections. Within this period, TWL values

Table 2 Classes of susceptibility to SLR with their related elevation ranges and corresponding potential coastal system response (modified after Di Paola et al. 2021)

Susceptibility class	Elevation range (h)	Coastal system response
Class S5 – very high susceptibility	h≤0 m	Areas expected to be below the projected mean sea level and thus very prone to be permanently inundated.
Class S4 – high susceptibility	0<h≤0.5 m	Areas prone to frequent temporary inundation which can lead to permanent morphological changes due to erosion and subsequent shoreline retreat.
Class S3 – medium susceptibility	0.5<h≤1 m	Areas prone to temporary inundation due to waves which can lead to permanent morphological changes due to erosion and subsequent shoreline retreat.
Class S2 – low susceptibility	1<h≤5 m	Areas prone to be temporarily inundated only due to high energy waves with consequent permanent morphological changes.
Class S1 – very low susceptibility	h>5 m	Areas with very low or null susceptibility with respect to future permanent sea inundation.

associated with the 10 and 100 years return period were used to represent both high and low frequency events respectively (Table 3). Taking into account the high-resolution elevation model, the study area was classified into five susceptibility classes, from "very low or no susceptibility" (Class S1) to "very high susceptibility" (Class S5), as defined in Table 3.

3.3.3 Evaluation of susceptibility to erosion

Susceptibility to erosion was assessed by accounting for the medium-term shoreline evolution characterizing the pocket beaches in the investigated bays. Anchor Bay was excluded from this assessment since this site lacks a well-developed beach. The shorelines were digitized from orthophotographs provided by the Maltese Ministry of Public Works and Planning (research and planning unit) covering the period 2004–2023. The images, with a spatial resolution of 0.15–0.25 m per pixel and a horizontal accuracy of approximately ± 0.5 m, were georeferenced. Furthermore, the shoreline referred to 2023 was digitized from Google Earth images downloaded in high quality (pixel density of 4800 × 3047) in order to improve the temporal resolution. The download was done by setting an altitude of 613 m and ensuring no image tilt. In total, six shorelines for each bay were digitalized.

The transition line between the beach sand and high-water level (wet-dry line) was chosen as the proxy for the digitization of the shorelines for different years. Then, the digitized shorelines were analysed in the Digital Shoreline Analysis System (DSAS), which is an extension to ESRI ArcGIS© (Thieler et al. 2009; Himmelstoss et al. 2024). This tool calculates the shoreline rate-of-change statistics starting from multiple historical shoreline positions. The analysis was performed by using transects drawn perpendicular to the baseline at a constant distance of 5 m. The uncertainty related to the mapping of shorelines was considered independent, uncorrelated and random as indicated by Borzì et al. (2021).

Additionally, orthophotos capturing storm conditions were not used for photointerpretation to prevent the influence of wave-induced runup that could compromise the analysis. Moreover, given that the investigated bays are characterized by microtidal conditions (Gauci et al. 2022 and references therein), tidal fluctuations are considered negligible and does not significantly affect the accuracy of shoreline detection.

The Linear Regression Rate (LRR) was used in this study to compute the shoreline change since it can use more than two shorelines. The resulting LRR values were classified into five susceptibility classes from "very low susceptibility" (Class S1), demarcated by very high accretion zones, to "very high susceptibility" (Class S5), demarcated by very high erosion zones (Oyedotun 2014; Darwish and Smith 2023), considering the LRR ranges indicated in Table 4. Finally, the highest susceptibility value in each bay was depicted as the erosion susceptibility level of the corresponding beach. In Table 4, the LRR values and

Table 3 Reference values used for the assessment of susceptibility to sea level rise and storm surges. Sea level projections correspond to the year 2100 under SSP1-2.6 and SSP5-8.5 scenarios, relative to the 1995–2014 baseline (IPCC 2023). Values in parentheses indicate the likely (17th–83rd percentile) range. Total water levels refer to the time interval 2071–2100 for 10-year and 100-year return periods

Parameters	Best-case scenario	Worst-case scenario
Long-term sea level projection (2100)	0.47 m (0.26–0.71 m) – SSP1-2.6	0.80 m (0.57–1.11 m) – SSP5-8.5
Long-term total water level (2071–2100)	0.76 m – 10-year return period	0.86 m – 100-year return period

Table 4 Shoreline change trends estimated based on the linear regression rate and related erosion susceptibility classes (cf. Luijendijk et al. 2018; Pantusa et al. 2022)

Shoreline trend	LRR (m/yr)	Erosion susceptibility
Erosion (high)	<-1	Class S5 – very high susceptibility
Erosion (low)	-0.5 to -1	Class S4 – high susceptibility
Stable	-0.5 to 0.5	Class S3 – medium susceptibility
Accretion (low)	0.5–1	Class S2 – low susceptibility
Accretion (high)	>1	Class S1 – very low susceptibility

Table 5 Rock-fall susceptibility classification based on the kinetic energy range (cf. Sarkar et al. 2024)

Rock fall susceptibility	Kinetic energy (kJ)
Class S1 – very low susceptibility	2711–60,972
Class S2 – low susceptibility	60,973–112,380
Class S3 – medium susceptibility	112,381–177,495
Class S4 – high susceptibility	177,496–266,601
Class S5 – very high susceptibility	266,602–439,671

the corresponding classification in terms of both shoreline trend ("erosion" and "accretion") and susceptibility levels are indicated.

3.3.4 Evaluation of susceptibility to rock falls

In order to identify rock-fall susceptibility zones, the Predictive Rockfall Tool—QPROTO was applied (cf. Castelli et al. 2021) to the bays and surrounding areas, which were considered potentially more exposed to this process due to higher presence of tourists and related facilities and infrastructures. A combination of geomorphological, structural and topographic analyses supported by detailed field surveys was used in order to identify the source areas considered for rock-fall simulations in QPROTO. In detail, potential rock-fall detachment zones were delineated based on slope threshold ($\geq 45°$) extracted from the LiDAR-derived DEM (Castelli et al. 2021; Sarkar et al. 2024). Subsequently, these source points were verified through field observations of persistent joints and lateral-spread fractures within the Upper Coralline Limestone plateau edges. Additional parameters, including block volume, block mass, detachment propensity, visibility distance, energy-line angle, and lateral spreading angle and were included as input in the model (Sarkar et al. 2024). Using QPROTO's cone method, run-out propagation cones were generated. Then, the resulting mean kinetic energy raster (kJ), incorporating the accounted variables within the energy balance framework and reflecting the potential impact energy associated with rock-fall intensity (Jaboyedoff et al. 2005; Scavia et al. 2020; Castelli et al. 2021), was classified into five susceptibility classes using geometrical interval classification method, from "very low susceptibility" (Class S1) to "very high susceptibility" (Class S5), as shown in Table 5. The raster was smoothed (3×3 kernel) and validated by comparison with field-observed boulder deposits.

The resulting breakpoints indicated in Table 5 correspond to statistically consistent intervals of kinetic energy, ensuring a balanced representation of low- and high-energy zones. The rock-fall modelled invasion were validated qualitatively by comparison with observed accumulation areas mapped during field surveys (Sarkar et al. 2024).

3.4 Phase 3: Coastal multi-risk assessment

Once all the data regarding susceptibility, exposure, and vulnerability were gathered and expressed in five classes, the final step of analysis includes combining and overlapping these data to evaluate the risk level and to zone out the investigated area under different risk classes. For the calculation of the multi-risk assessment, all the above-mentioned informative layers were combined by using the formula depicted by Eq. 1 (modified after Armaroli and Duo 2018).

$$\text{Coastal Risk Index} = \sqrt[n]{(C_{Sus} * C_{Exp} * C_{Vuln})} \quad (1)$$

where, ^{n} represents the number of indicators, C_{Sus} symbolizes the susceptibility value related to SLR, storm surge, rock fall and erosion, C_{Exp} represents the exposure value related to physically exposed elements (land use, transport, and utilities), and C_{Vuln} represents the value of the coastal vulnerability related to tourism and environment.

Finally, the Coastal Risk Index is classified and mapped into four risk classes, ranging from "low risk" (Class R1) to "very high risk" (Class R4) as shown in Table 6. Due to the fact that susceptibility to permanent increase in sea level can be assessed based on projections related to two different climate scenarios (i.e., SSP1-2.6 and SSP5-8.5) and TWL is associated with different return periods (i.e., 10 and 100 years), the final risk for the year 2100 is expressed as best- and worst-case conditions.

4 Results

The outcomes of the analyses carried out in this study are provided in form of maps that display the exposure (land use, transport and utilities), vulnerability (tourism and environmental), susceptibility (SLR, storm surge, erosion and rock falls), and risk levels estimated for the north-west coast of Malta.

4.1 Outcome of coastal exposure and vulnerability assessment

The assessment of the physical exposure was conducted using the procedure described in Sect. 3.2, which allowed for delimiting areas with varying exposure classes and calculating their extent. The resulting exposure maps are presented in Fig. 5, with corresponding quantitative data summarised in Table 7. Overall, the results reflect a heterogeneous spatial distribution of exposure levels across the study area, ranging from very low to very high. Highly exposed areas were identified in the northern parts of Anchor Bay and Golden Bay. These sectors are characterised by a high density of tourist and leisure facilities (e.g., hotel, amusement park and other entertainment facilities) and infrastructures. The coastal sector of Gnejna Bay shows localised areas of very high exposure associated with the presence of

Table 6 Coastal multi-risk classification

Coastal multi-risk Class	CRI range	Risk level
Class R1	CRI<=1.5	Low risk
Class R2	1.5<CRI<=2.5	Medium risk
Class R3	2.5<CRI<=3.5	High risk
Class R4	CRI>3.5	Very high risk

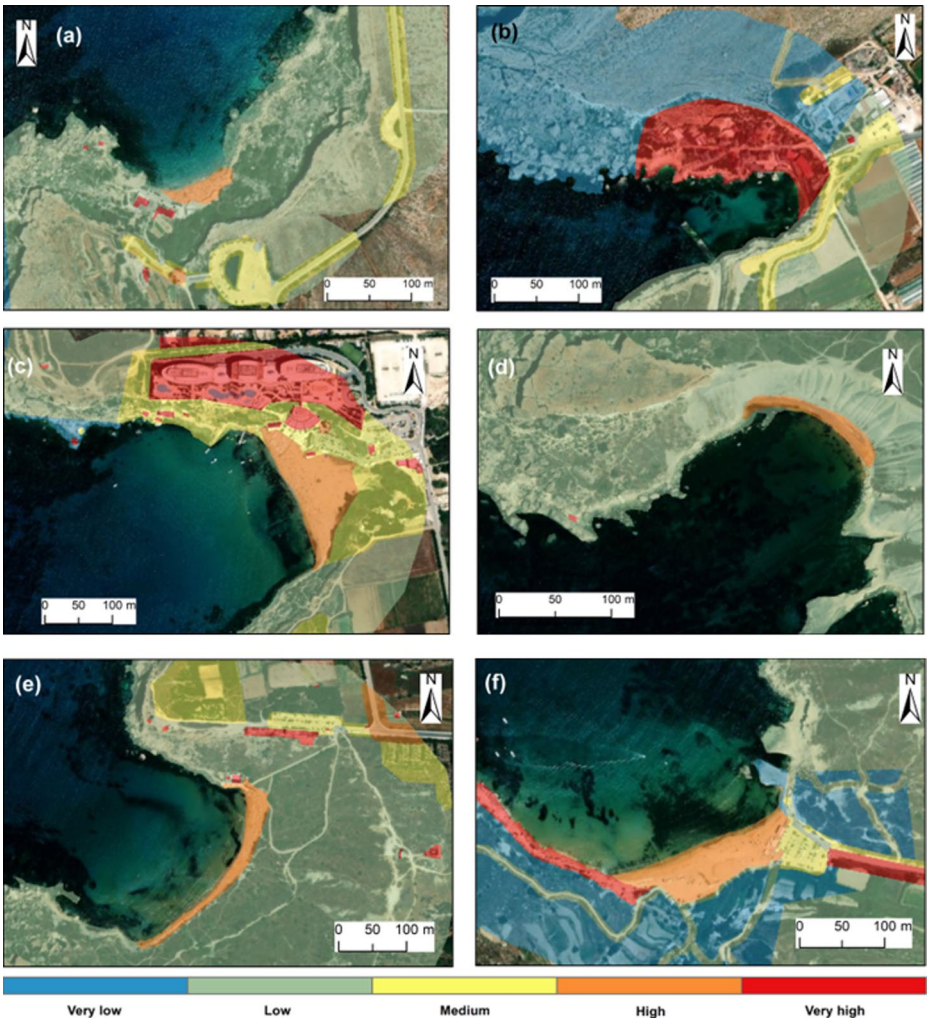

Fig. 5 Exposure maps resulting from data overlay of the physical indicators (land use, transport and utilities). **a** Paradise Bay, **b** Anchor Bay, **c** Golden Bay, **d** Qarraba Bay, **e** Ghajn Tuffieha Bay, and **f** Gnejna Bay

Table 7 Results of the exposure assessment showing the areal extent and percentage of each exposure level class derived from the overlay and aggregation of the physical indicators (land use, transport network, and utilities)

Exposure level	Surface (km^2)	Surface (%)
Very low exposure	1.57	42.94
Low exposure	1.76	47.97
Medium exposure	0.16	4.40
High exposure	0.08	2.23
Very high exposure	0.09	2.46

boat houses and small coastal structures. This pattern indicates that anthropogenic pressure and built-up land cover are the main determinants of high exposure in the investigated area.

Low level of exposure characterised the less anthropised coastal sectors surrounding Paradise Bay, Ghajn Tuffieha Bay, and Qarraba Bay, which mainly host agricultural land and natural sclerophyllous vegetation. However, a medium exposure level prevails in some patches where the trails and footways connecting the beaches to the cliffs are located. The inner sectors of the study area present very low exposure, being dominated by bare rock outcrops and minimal human presence.

Selected indicators, reflecting both tourism and environmental characteristics of the investigated area, allowed for a detailed assessment of vulnerability in line with established frameworks (Maanan et al. 2018; Scott et al. 2019).

The numerical values assigned to each of the tourism and environmental vulnerability indicators are summarised in Table 8. The aggregation of these indicators resulted in the identification of distinct tourism and environmental vulnerability levels for the investigated sites (Fig. 6). Ghajn Tuffieha Bay and Golden Bay exhibit very high vulnerability, followed by Paradise Bay with high vulnerability. These results reflect the prominent tourist vocation of these sites, evidenced by the high number of online photographs and reviews, as well as their environmental importance linked to the presence of natural protected areas. The remaining sites display medium to very low tourism and environmental vulnerability, mainly due to their reduced accessibility and limited tourist facilities, which in turn constrain tourist pressure. In these areas, the presence of only one natural protected site further contributes to lower the overall vulnerability.

4.2 Outcomes of the coastal susceptibility assessment

The susceptibility analysis for local permanent SLR in 2100 under two different climate scenarios allowed to classify the area under investigation into five susceptibility classes, as shown in Table 9; Fig. 7. For what concern the susceptibility analysis due to TWL increases, quantitative results for the 10 and 100 years return periods are reported in Table 10 and mapped in Fig. 8 (elaborated by considering the end-century 100 years return period).

The outcomes of susceptibility assessment (inundation and storm surge) depict that most of the investigated sites are safe zones (Class S1) since these areas have an elevation above 5 m a.s.l. Only approximately 1% of the investigated territory falls under the high susceptibility class (Class S4) mainly corresponding to low-lying coastal sectors below 1 m a.s.l.

Table 8 Results of the assessment of tourism and environmental vulnerability, based on the quantitative indicators derived from Google data and the number of natural protected areas

Sites	No. of reviews from Google	No. of pictures from Google	No. of natural protected sites	Tourism vulnerability	Environmental vulnerability
Paradise Bay	63,138	3	1	3	1
Anchor Bay	28,196	5	1	2	1
Golden Bay	409	40	2	3	3
Qarraba Bay	176	2	1	1	1
Ghajn Tuffieha Bay	2468	4	3	1	5
Gnejna Bay	15	1	1	1	1

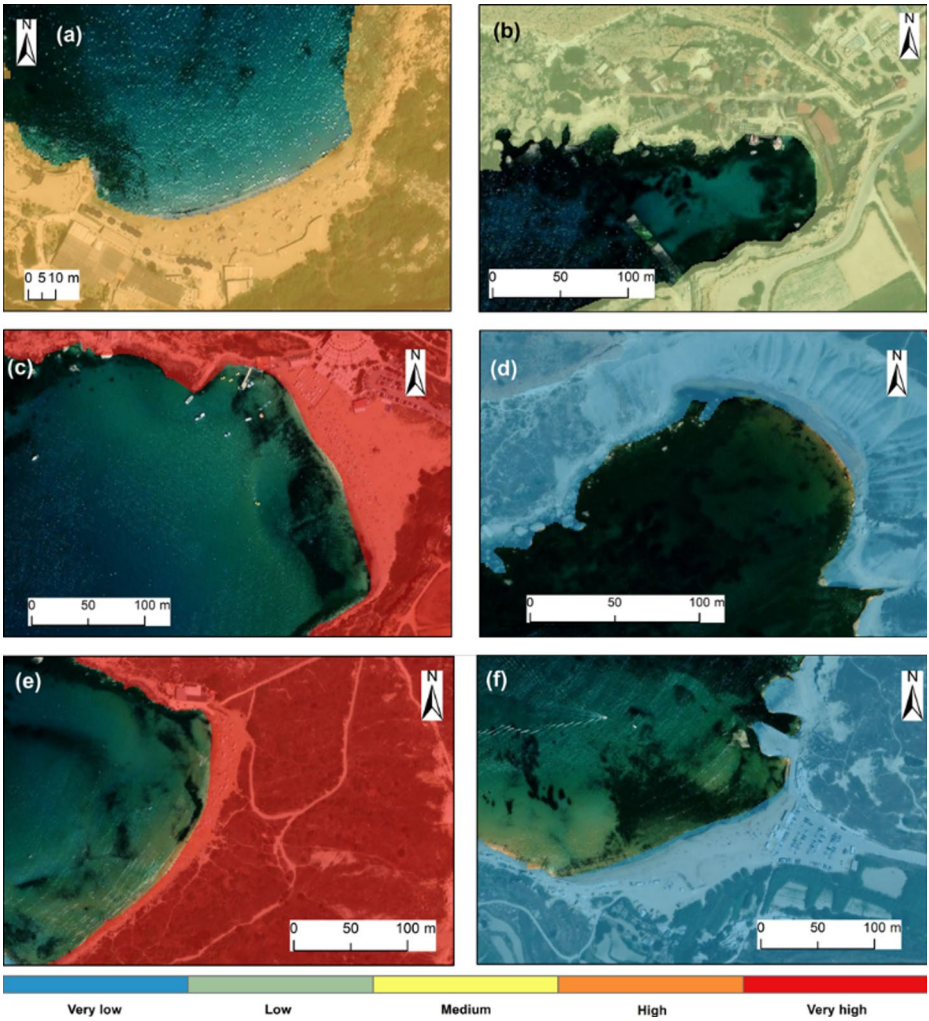

Fig. 6 Tourism and environmental vulnerability maps resulting from data overlay of the tourism and environmental indicators. **a** Paradise Bay, **b** Anchor Bay, **c** Golden Bay, **d** Qarraba Bay, **e** Ghajn Tuffieha Bay, and **f** Gnejna Bay

Despite their limited spatial extent, these highly susceptible areas are located in correspondence of the main bays, which represent key sites of economic, touristic and environmental value, and should therefore be given greater attention. With respect to the extent of areas potentially affected by permanent submersion due to SLR, the affected surface is projected to increase by approximately 25%, from 0.004426 km^2 under the most favourable climate scenario to 0.005554 km^2 under the most adverse climate scenario. Conversely, the areas exhibiting high and very high susceptibility to the expected TWL remain largely unchanged when comparing the 10- and 100-year return periods, with only a 16% increase observed for class S5.

Table 9 Spatial extension (expressed as km^2 and %) of the areas falling in the inundation susceptibility classes S1-S5 due to SLR for different local sea level projections in 2100 under the best-case (SSP1-2.6) and worst-case scenarios (SSP5-8.5)

Susceptibility (SLR)	SSP1-2.6		SSP5-8.5	
	Area (km^2)	Area (%)	Area (km^2)	Area (%)
Class S1 – very low susceptibility	3.083065	84.24	3.083013	84.21
Class S2 – low susceptibility	0.230222	6.29	0.230239	6.29
Class S3 – medium susceptibility	0.304359	8.32	0.304361	8.31
Class S4 – high susceptibility	0.037928	1.04	0.037833	1.03
Class S5 – very high susceptibility	0.004426	0.12	0.005554	0.15

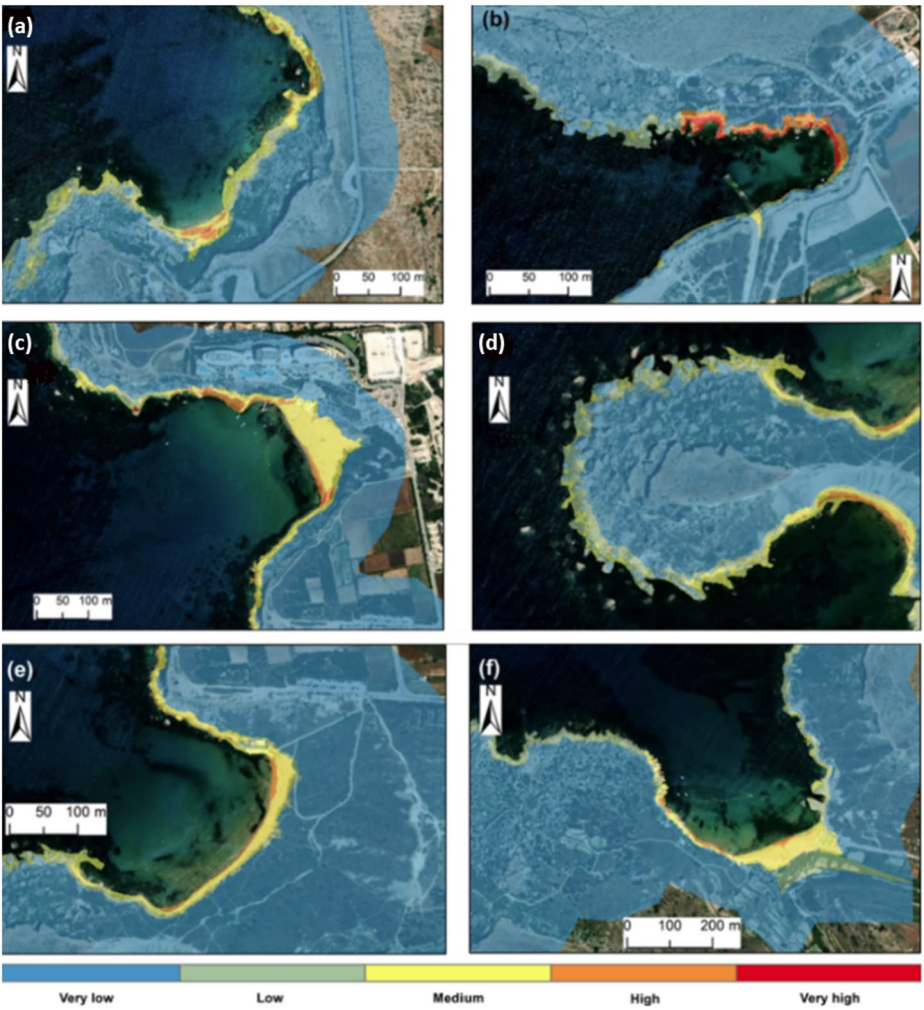

Fig. 7 Inundation susceptibility (Classes S1-S5) of bay areas due to SLR. Mapping is based on the local projection in 2100 under the worst-case climate scenario (SSP5-8.5). **a** Paradise Bay, **b** Anchor Bay, **c** Golden Bay, **d** Qarraba Bay, **e** Ghajn Tuffieha Bay, and **f** Gnejna Bay

Table 10 Spatial extension (expressed as km² and %) of the areas falling in susceptibility classes S1-S5 due to TWL with a 10 and 100 years return period in 2100

Susceptibility (TWLSLR)	10 years return period		100 years return period	
	Area (km^2)	Area (%)	Area (km^2)	Area (%)
Class S1 – very low susceptibility	3.42103	93.47	3.435043	93.85
Class S2 – low susceptibility	0.118194	3.23	0.101469	2.77
Class S3 – medium susceptibility	0.062507	1.71	0.062507	1.71
Class S4 – high susceptibility	0.048222	1.32	0.049307	1.35
Class S5 – very high susceptibility	0.010047	0.27	0.011674	0.32

The outputs obtained from the analysis of SLR susceptibility under the best-case scenario (SSP1-2.6) and for shorter return periods (i.e., 10 years) have not been presented as figures of the paper for graphical reasons and to ensure a concise presentation of the results.

The results of shoreline change obtained using the DSAS tool showed that the pocket beaches in the bays along the north-west coast of Malta are currently characterised by an overall stability (Fig. 9). Localised and intermittent erosion occurs in certain sectors, reflecting the complex geological and geomorphological setting of the area. The shoreline classifications for each investigated bay based on the LRR results and on the corresponding susceptibility levels are depicted in Figs. 9 and 10, respectively. Although Ghajn Tuffieha Bay depicts a predominant medium level of erosion (Fig. 9b), it falls under susceptibility Class 4 (Fig. 10b) since the highest value in this bay is 4 (high susceptibility). This classification is further supported by Farrugia (2008), whose analysis on shoreline changes from 1939 to 1993 confirmed that Ghajn Tuffieha Bay is highly susceptible to erosion.

The results of rock-fall runout susceptibility highlight that Gnejna Bay includes the maximum percentage area under high runout probability level (29.3%) followed by Anchor Bay (27.9%) and Golden Bay (27.5%), as shown in Fig. 11. The spatial pattern of rock-fall susceptibility is mainly influenced by the geomorphological and structural setting of the investigated area. In particular, the presence of numerous persistent discontinuities within the Upper Coralline Limestone plateaus which are bordered by highly-jointed sub-vertical cliffs favour extensive rock-mass fragmentation and potential block detachments (Devoto et al. 2020). Beneath the plateaus, Blue Clay steep slopes enhance downslope propagation. A considerable part of Il-Qarraba caprock, overlooking the Qarraba Bay, falls under medium to high probability, consistent with the geomorphological and structural setting depicted above. Such areas are more prone to failures as a consequence of extreme precipitation and increased storm-surge frequency in the Maltese Islands. The spatial distribution of runout zones aligns well with field evidence and recorded events, including, for instance, the rock falls affecting the Il-Qarraba caprock on 26th November 2011 and northern cliff of Anchor Bay event on 9th February 2023 during a violent storm.

The inner parts of the bays represent medium to low rock-fall runout probability zones, being located farther away from the rock-fall source areas.

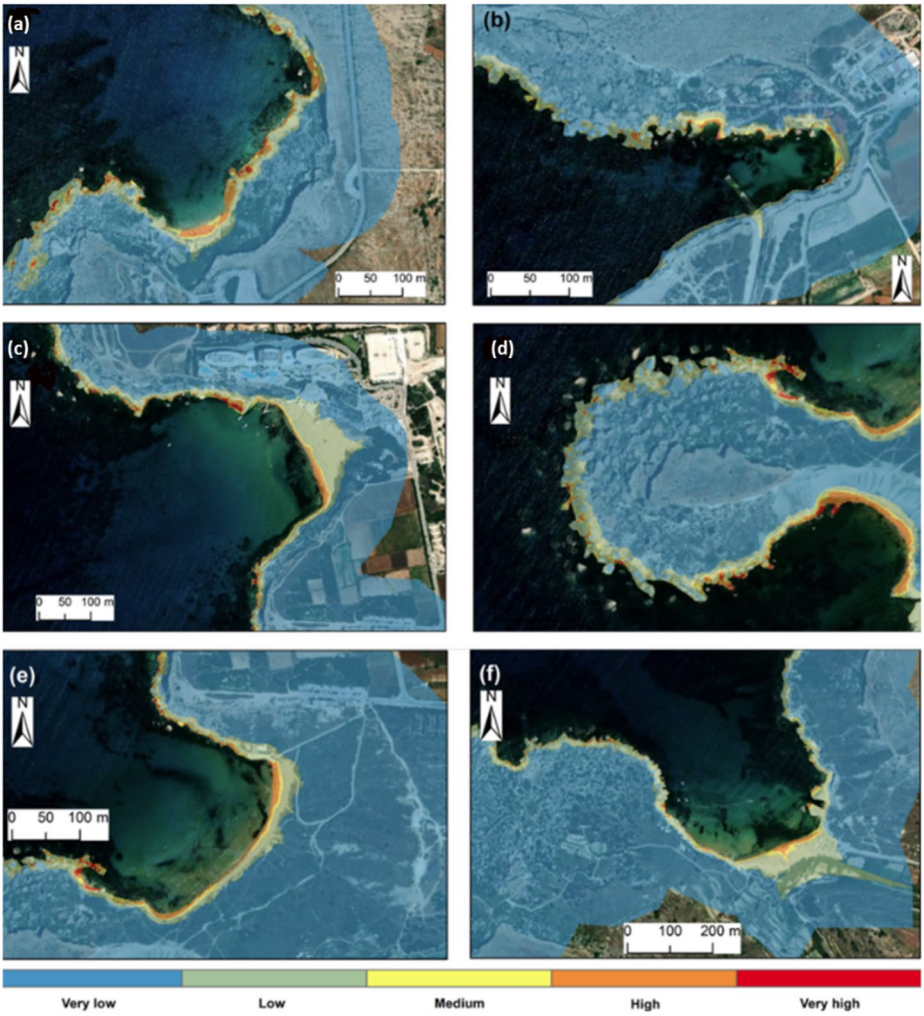

Fig. 8 Inundation susceptibility (Classes S1-S5) of bay areas due to storm surge. Mapping is based on the TWL end-century data with 100 years return period. **a** Paradise Bay, **b** Anchor Bay, **c** Golden Bay, **d** Qarraba Bay, **e** Ghajn Tuffieha Bay, and **f** Gnejna Bay

4.3 Outcome of coastal multi-risk assessment

The combination of coastal exposure, vulnerability and susceptibility to SLR, storm surge, erosion and rock fall allowed the estimation and mapping of multi-risk levels for the investigated coastal sector. Specifically, the multi-risk analysis was performed for the long-term period by considering SLR projections in 2100 under two climate scenarios and TWL for both 10 and 100 years return period. Quantitative results relative to best- and worst-case conditions are shown in Fig. 12; Table 11.

The total extent of the area with high and very high risk shows an increase higher than 145%, passing from 0.095405 km^2 (under the best condition) to 0.23542 km^2 (under the

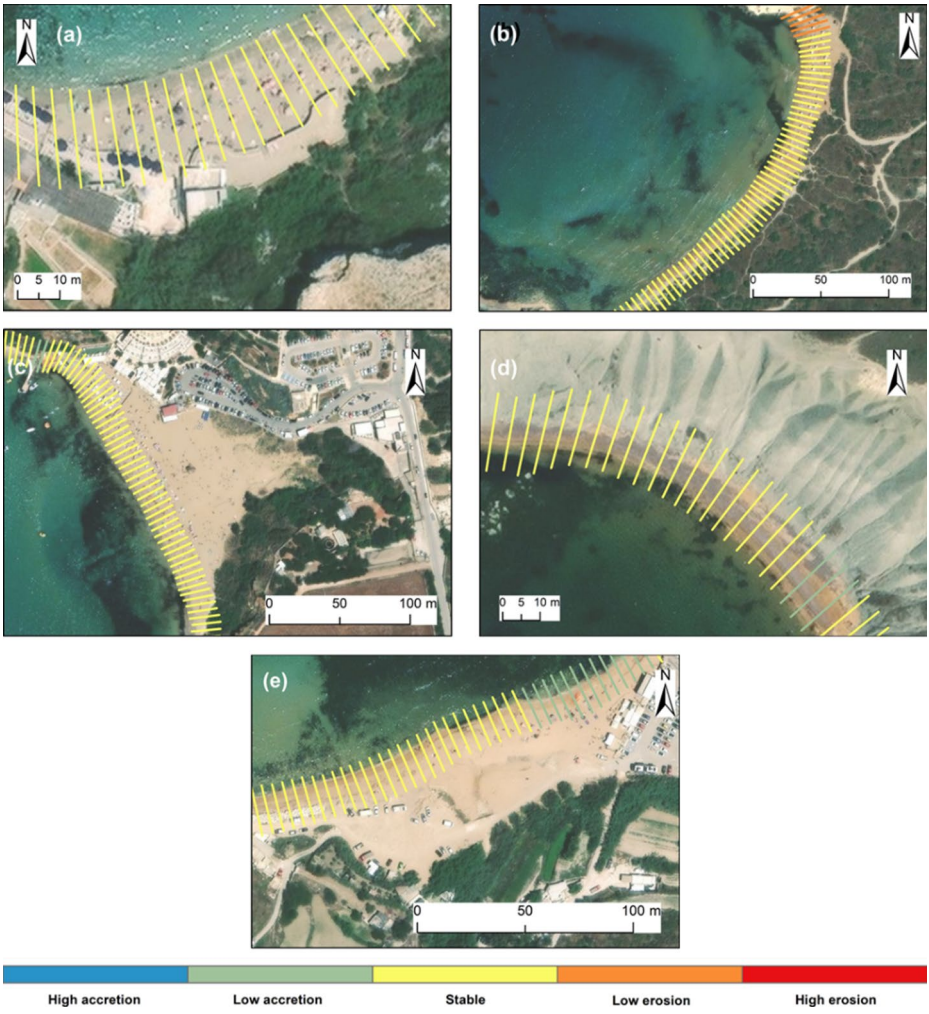

Fig. 9 Maps showing shoreline change over the period 2004–2023 based on the Linear Regression Rates and shoreline classification reported in Table 4. **a** Paradise Bay, **b** Ghajn Tuffieha Bay **c** Golden Bay, **d** Qarraba Bay, and **e** Gnejna Bay. The length of the coloured transects shown in "**a**–**e**" was set by using the DSAS software and it does not represent the extent of the beach affected by erosion or accretion

worst condition). This means that, accounting for the current asset of natural and anthropic exposed elements and under the best-case conditions, approximately 10% of the investigated areas within 1 m a.s.l. can be considered at risk for the year 2100 (including classes R3 and R4). This value increases up to 21% under the worst-case scenarios, with 3% of the investigated area in Class R4 and 18% in Class R3.

In detail, the risk assessment process identified six hotspot areas (Paradise Bay, Anchor Bay, Golden Bay, Ghajn Tuffieha Bay, Qarraba Bay and Gnejna Bay), as shown in Fig. 12. These locations are particularly prone to the coupled impacts of sea level rise, and its associated effects, and rock falls. Golden Bay, Ghajn Tuffieha Bay and Anchor Bay are characterised by high-risk level. This is due to (i) high exposure and vulnerability levels prevailing

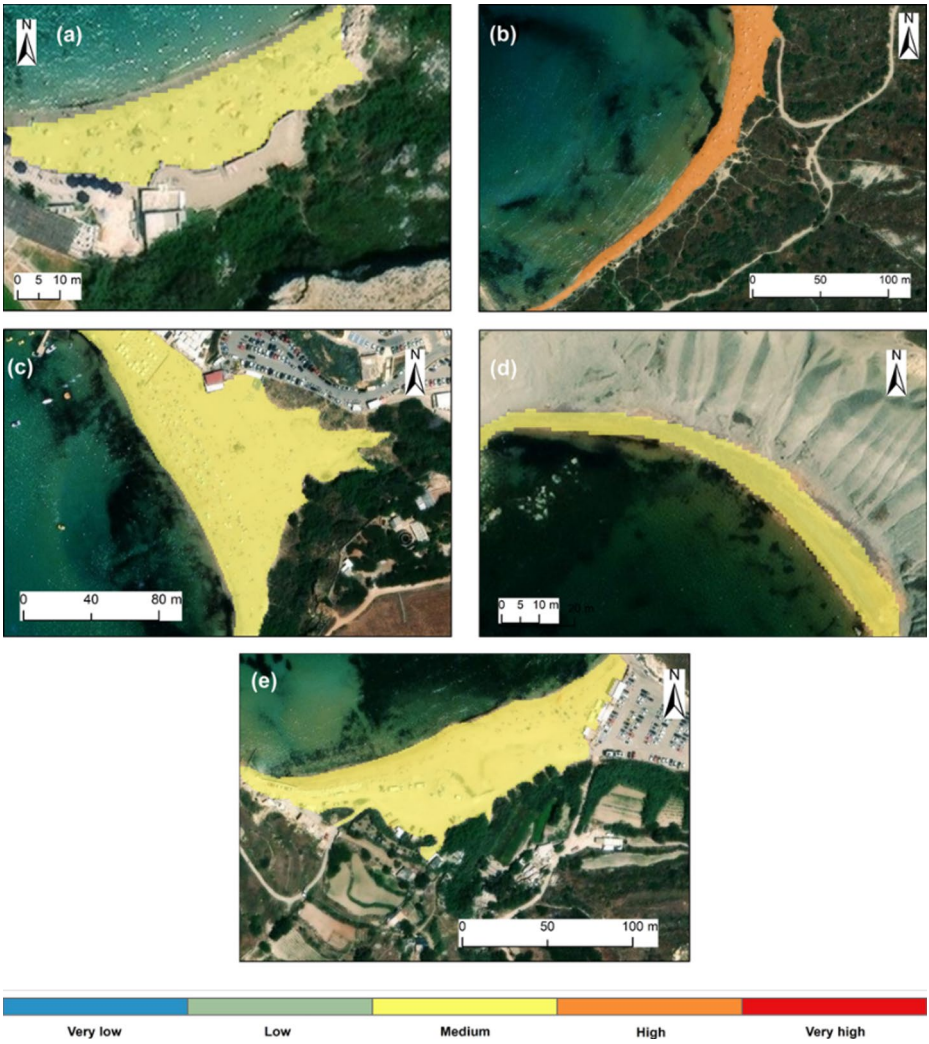

Fig. 10 Erosion susceptibility maps. **a** Paradise Bay, **b** Ghajn Tuffieha Bay **c** Golden Bay, **d** Qarraba Bay, and **e** Gnejna Bay

along these bays influenced by the presence of beaches surrounded by tourism and entertainment spots, (ii) more tourism pressure indicated by high number of photos and reviews uploaded, and (iii) the presence of natural protected areas. Susceptibility levels due to SLR along most parts of Anchor Bay are high, influencing the risk level of this area. Paradise Bay shows a prevalent low to medium level of risk, influenced by low exposure along this area due to the presence of sclerophyllous vegetation and rocky ground around the beach. The medium susceptibility level due to erosion along the beach also influences the risk level of this area. Furthermore, many stretches of Qarraba Bay show low risk levels since this zone has very low tourism and environmental vulnerability levels. The low risk level along cer-

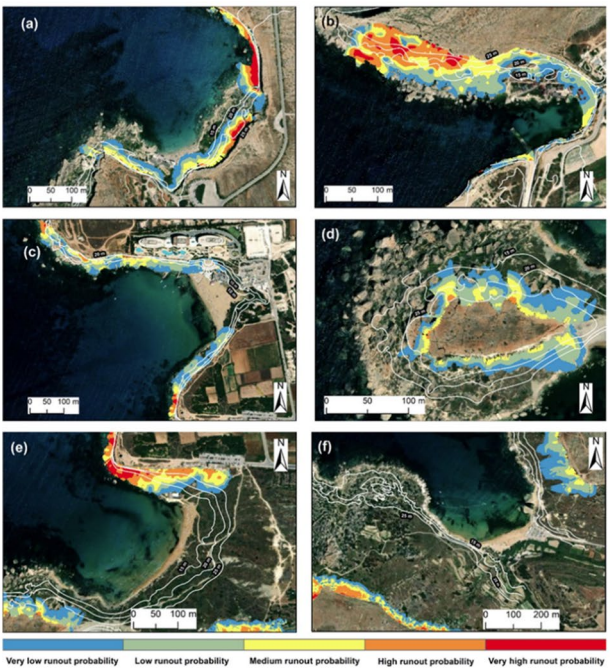

Test site	Very low (m²)	Surface (%)	Low (m²)	Surface (%)	Medium (m²)	Surface (%)	High (m²)	Surface (%)	Very high (m²)	Surface (%)	Total runout area (m²)
Paradise Bay	6158	28.0	2538	11.5	4770	21.7	5615	25.5	2912	13.3	21,991
Anchor Bay	6163	18.8	5839	17.8	7775	23.7	9142	27.9	3884	11.8	32,801
Golden Bay	5196	19.1	4069	14.9	8244	30.2	7493	27.5	2273	8.3	27,273
Ghajn Tuffieha Bay	6024	26.5	3638	16.0	6441	28.3	5700	25.1	927	4.1	22,729
Il-Qarraba promontory	2906	17.1	3554	20.9	4257	25	4398	25.9	1887	11.1	17,001
Gnejna Bay	16,067	21	12,706	16.6	21,466	28	22,466	29.3	3954	5.1	76,657

Fig. 11 Rock-fall runout susceptibility zones and percentage of surface area under each zone for the investigated sites (modified after Sarkar et al. 2024). **a** Paradise Bay, **b** Anchor Bay, **c** Golden Bay, **d** Qarraba Bay, **e** Ghajn Tuffieha Bay, and **f** Gnejna Bay

tain parts of Gnejna Bay is influenced by very low tourism and environmental vulnerability levels prevailing along this stretch of coast.

5 Discussion

The results of the exposure, vulnerability and susceptibility analyses carried out in this study highlight that the north-west coast of the island of Malta can be considered as significantly prone to the impacts of multiple climate-related coastal hazards, such as SLR, storm surges, erosion and rock fall. The latter is also favoured by the geomechanical properties of the rock units outcropping in the investigated coastal sector.

As arises from the results obtained through the susceptibility analysis under two different climate scenarios, the increase in areas characterized by very high susceptibility is lower than 10%, passing from 1,44 to 1,5 m^2, under the SSP1-2.6 and SSP5-8.5, respectively. Similar results are also obtained from the analysis of the TWL increases associated with two

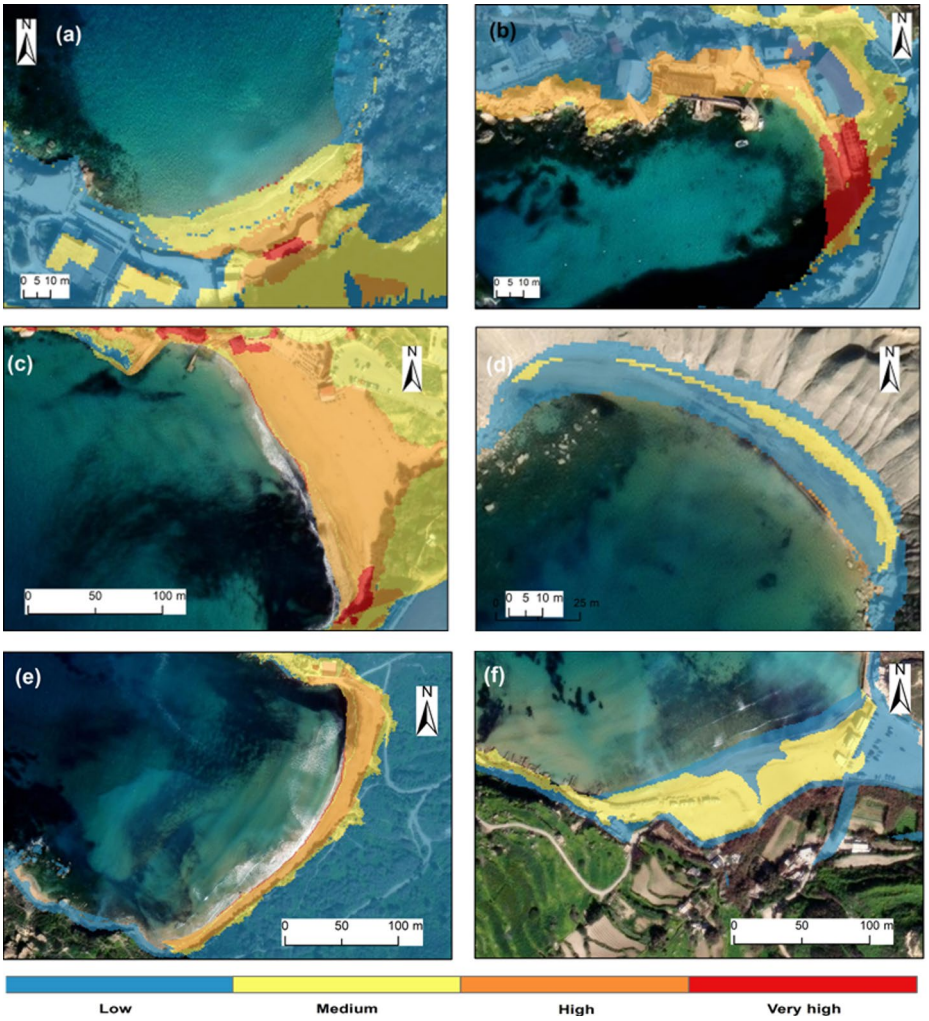

Fig. 12 Multi-risk maps of the investigated sites based on the worst-case conditions (SLR SSP5-8.5 and TWL with 100 years return period). **a** Paradise Bay, **b** Anchor Bay, **c** Golden Bay, **d** Qarraba Bay, **e** Ghajn Tuffieha Bay and **f** Gnejna Bay

different return periods, passing from 3.2 to 3.4 m^2. As a consequence, also the increase in the extent of the high and very high risk levels is quite limited (passing from 18 m^2 under the best-case condition to 45 m^2 under the worst-case condition).

These results indicate that the differences in projected risk levels between the best- and worst-case conditions estimated for the year 2100 are relatively minor, indicating low sensitivity of the applied methodology to the scenarios' variability. This outcome suggests that the results are mainly driven by the spatial variability of the indicators used in the risk assessment, which may limit the capability of the approach to capture the full range of climate-related uncertainties. Future analyses could benefit from probabilistic modelling approaches in order to enhance sensitivity and robustness in scenario-based risk assessment.

Table 11 Spatial extension (expressed as km^2 and %) of the areas with different multi-risk level in 2100 under the best-case (SLR rise for the SSP1-2.6 and TWL with 10 years return period) and worst-case scenarios (SLR rise for the SSP5-8.5 and TWL with 100 years return period)

Risk levels	Best-case condition (SLR SSP1- 2.6 + TWL 10 years return period)		Worst-case condition (SLR SSP5- 8.5 + TWL 100 years return period)	
	Area (km^2)	Area (%)	Area (km^2)	Area (%)
Low	2.64763	72.32	2.576636	70.40
Medium	0.917965	25.07	0.847944	23.17
High	0.066489	1.82	0.206713	5.65
Very high	0.028916	0.79	0.028707	0.78

From the methodological point of view, the analyses carried out in this research are in line with the most used indicator- and GIS-based approaches (Rizzo et al. 2025). According to previous applications (Beccari 2016), the physical, tourism and environmental indicators exploited for the evaluation of each parameter used for the risk assessment were equally weighted, implying that each indicator had the same impact on the final risk evaluation. The lack of a standardized or empirically justified weighting method could cause discrepancies between studies, making cross-validation challenging. Based on the above assumptions, it is clear that the application of the index-based approach for the multi-risk analysis should be made considering its methodological limitations. These include the reliance on parameters evaluated based on expert judgement, which can introduce a degree of subjectivity, and the mismatch in resolution between available datasets and site scale, which can affect the spatial accuracy of the outputs, specifically in complex coastal settings with significant local variations.

To ensure that the proposed methodological approach could be easily transferable to other similar coastal sectors, the semi-quantitative analyses here proposed are based on the assumption that data obtained from freely accessible web platforms can be reliably used to quantify the parameters considered in the study.

For what concerns the evaluation of each parameter composing the risk, it is worth to note that the estimation of coastal exposure of the assets prone to the expected impacts of climate change provide a basis for usable science for managing coastal risks (Kopp et al. 2019).

The assessment of susceptibility to SLR and TWL is based on the exploitation of elevation data that are widely available and easy to obtain for many regions allowing faster, low-cost analysis. Despite knowing the fact that sophisticated model-based methods are more used in recent times for such analysis (Androulidakis et al. 2023; Mel et al. 2023; Kefi et al. 2024), this research made use of traditional elevation-based approach, providing a first level of susceptibility assessment and highlighting the areas that require further detailed modelling analysis (Dasgupta et al. 2009; Santos et al. 2024).

It is important to underline that, even if the TWL can be regarded as an extreme-value indicator providing a basis for research aimed at evaluating sea level fluctuation, coastal flooding and coastal erosion at a large scale, its resolution in spatial variability could represent a criticality for site-specific sites. In fact, although Copernicus CDS provides consistent, freely accessible and quality-controlled reanalysis data, TWL projections are characterized by a horizontal resolution relatively coarse (approximately 11 km) for representing very local scale coastal variability and localized storm-surge effects, which may limit the possi-

bility of capturing the local storm-surge variability at the bay scale. Nevertheless, the overall patterns of susceptibility remain representative for regional scale analysis.

The outcomes of susceptibility assessment to SLR and storm surge in the form of maps and graphical representation align with the results of studies in the Mediterranean basin, which face significant coastal implications from SLR and associated processes (as highlighted by recent studies, including Ferreira et al. 2018; Di Paola et al. 2021; Rizzo et al. 2022; Sarkar et al. 2022; Scardino et al. 2022; Thiéblemont et al. 2024).

The study's approach for mapping erosion susceptibility is consistent with numerous studies dealing with coastal susceptibility to erosion which are based on the exploitation of index-based methods (cf. Rizzo et al. 2018; Tursi et al. 2023, 2025). In relation to statistics used for erosion susceptibility, the Linear Regression Rate (LRR) tends to underestimate the rate of change and is therefore vulnerable to the uncertainties mainly related to the detection of instantaneous shoreline positions (Dolan et al. 1991), which could be affected by local tide and wave setup. To mitigate these limitations, all the available shorelines from different time periods were considered in the erosion susceptibility analysis, allowing for a more reliable medium-term assessment of shoreline evolution. In the investigated bays, this method enabled a consistent evaluation of shoreline retreat over time, regardless of the varying extents of the six pocket beaches, the widest of which does not exceed 82 m.

Regarding tidal values, the investigated coastal sites are subject to microtidal conditions, with a tidal range not exceeding ± 0.30 m (Gauci et al. 2022 and references therein). Furthermore, considering that in the Google Earth Pro User Guide the exact time of image acquisition is not provided as metadata, it is not possible to determine the precise tidal stage at the time each individual image was captured. Despite its limitations, the method continues to be widely used in both scientific and technical studies for assessing recent shoreline displacements since it is based on simple computational statistical concepts.

The rock-fall susceptibility analysis was performed considering a systematic approach as illustrated in Sarkar et al. (2024). This procedure involves processing of GIS-based topographic information in order to identify a set of rock-fall source points. The outputs of the model were then validated by in-situ field surveys, showing that rock-fall invasion zones observed in the field are largely comparable to those generated by the model.

The overall aim of this study was to develop a baseline assessment by integrating exposure, susceptibility and vulnerability data, in order to provide stakeholders and planning authorities with knowledge-based maps identifying the areas at risk. The findings of this study are aligned with the outcomes of the work by Formosa (2015), where the entire Maltese coast was studied with respect to fixed values of future sea levels. Also, in the latter study, the tourism and recreational areas were included in the most exposed zones under all the considered sea levels.

In this context, our study identifies different risk levels based on best- and worst-case scenarios for the north-west coastal sectors of Malta, providing a means of comparison with the sea levels considered for adaptation measures (50 cm in 2050 and 100 cm in 2100) by Ministry for Rural Affairs and the Environment in 2004 as depicted in the Climate Change Post (2024).

This study does not consider local factors like subsidence or uplift contributing to future sea level variation. Such local factors are commonly taken into consideration in many coastal sectors of the Mediterranean Sea (Tosi et al. 2002, 2016; Da Lio and Tosi 2018;

Di Paola et al. 2021; Scardino et al. 2022). However, according to Serpelloni et al. (2007, 2013), there are no significant vertical tectonic movements affecting the Maltese Islands.

The method used in the study is cost-effective since all the required data are managed and processed in a GIS environment, making results easily communicable and interpretable. The display of outputs in the form of spatial mapping effectively communicates the risk in local contexts and, through co-construction and validation with stakeholders, can support the implementation of suitable measures for adaptation, resilience to climate change, and sustainable development. This approach of climate risk assessment provides a strong connection between local-level susceptibility and vulnerability analysis and national policy-making. The applied method and achieved results in such terms are uncommon in Maltese policy perspectives. This is because no type of strategy for adaptation or defence to sea level rise has been planned to date.

The applied index-based approach suits well for the assessment of potential impacts of climate-related risks (Reimann et al. 2018; Makris et al. 2023), allowing the preliminary identification of coastal areas characterised by high risk and therefore requiring further consideration. It provides a consistent framework for the estimation and spatial representation of risk levels across regional and local scale. However, the lack of a standardized or empirically justified weighting method could cause discrepancies between studies, making cross-validation challenging. Moreover, resolution mismatches between datasets and site scale might affect the spatial accuracy of the output, specifically in varied coastal settings with significant local variations. To fill the gap due to the lack of historical data on hazardous events, a quantitative approach was used for the susceptibility and vulnerability analysis, which provides a first-level zonation of the investigated territory. This approach can be crucial for targeting economic resources and technological investments.

6 Conclusions

The study represents a first attempt to evaluate coastal risks associated with the main climate-related processes in the north west coast of the island of Malta. The study enabled the assessment and zonation of coastal susceptibility, exposure and vulnerability related to the above-mentioned processes and the assessment of the coastal multi-risk level for the year 2100 under two climate scenarios (best- and worst-case conditions). The study is based on the exploitation of index-based methods, allowing the identification of coastal sectors for which more advanced modelling analyses are required. The results are provided in the form of maps that could be used for effective communication of coastal risk. Results highlighted that the investigated coastal sector can be considered prone to be affected by the combined effects of the processes taken into account. In particular, the pocket beaches located in the main bays within the investigated coastal stretch can be considered as hotspots due to their geomorphological setting (low topography, absence of rivers for sediment inputs, presence of unstable boulders) and to their high tourist exploitation during all the year.

Being mainly occupied by abandoned agricultural lands and bare rock outcrops and presenting a topographic elevation higher than 5 m a.s.l, approximately 70% of the investigated area is characterized by low-risk under the accounted scenarios. Nevertheless, the remaining portion of the coastline would require attention through adaptive planning and policy

actions in order to safeguard the infrastructure, touristic amenities, and natural habitats from the potential impacts of climate change.

While this method allows to zone out the most vulnerable coastal sectors of Malta, providing a more thorough risk assessment and guidance for future policy action, further investigation is required to validate the performance of this multi-risk assessment approach. Thus, future analysis will focus on the assessment of the accuracy of such methods through comparison of different methodologies in order to ensure more effective risk assessment also considering the cascading effect of the accounted processes. Further investigations should also consider the influence of land-use change and urban development on exposure and risk patterns.

Finally, beyond the scope of this study, general response strategies to address the identified coastal risks may include relocation of vulnerable assets, protection through engineering or nature-based solutions, accommodation by adapting existing uses, and prevention using improved planning. Such actions closely align with the response modalities (Molina et al. 2020), and integrated coastal zone management principles in order to ensure long-term resilience and environmental sustainability.

Acknowledgements This paper and related research have been conducted during and with the support of the Italian interuniversity PhD course in sustainable development and climate change (www.phd-sdc.it). The research was also supported by the RETURN Enlarged Partnerships under the National Recovery and Resilience Plan (NRRP), Mission 4, Component 2, Investment 1.3 funded by the European Union—NextGenerationEU (RETURN project "Multi-risk science for resilient communities under a changing climate", no. PE00000005, CUP B53C22004020002, Author contribution: A. Rizzo).

Author contributions All authors contributed to the study conception and design. The methodology applied was developed and implemented by Nabanita Sarkar, Angela Rizzo and Vittoria Vandelli. Material preparation, data collection and analysis were performed by Nabanita Sarkar. The first draft of the manuscript was written by Nabanita Sarkar and all authors contributed to writing, reviewing and editing the further versions of the manuscript. Visualization (preparation and design of figures and graphical data representations) was carried out by Nabanita Sarkar with the assistance of Vittoria Vandelli. Mentoring, supervision, and leadership responsibility for the execution of research activities were provided by Angela Rizzo. The planning, execution, and overall coordination of the research activities were managed by Mauro Soldati and Angela Rizzo. The acquisition of resources and funding was managed by Mauro Soldati. All authors read and approved the final manuscript.

Declarations

Conflict of interest The authors declare that they have no conflict of interest.

References

Abouelnasr MM, Elselmy AS (2024) Medicanes and its metrological effects in the Mediterranean Sea: case study of Medicane Ianos. Arab Academy for Science, Technology, and Maritime Transport. The International Maritime and Logistics Conference Marlog 13 Towards Smart Green Blue Infrastructure

Amores A, Marcos M, Carrió DS et al (2020) Coastal impacts of Storm Gloria (January 2020) over the northwestern Mediterranean. Nat Hazards Earth Syst Sci 20(7):1955–1968. https://doi.org/10.5194/nhess-20-1955-2020

Androulidakis Y, Makris C, Mallios Z et al (2023) Storm surges and coastal inundation during extreme events in the Mediterranean Sea: the IANOS Medicane. Nat Hazards 117(1):939–978. https://doi.org/10.1007/s11069-023-05890-6

Antonioli F, Anzidei M, Amorosi A et al (2017) Sea-level rise and potential drowning of the Italian coastal plains: flooding risk scenarios for 2100. Q Sci Rev 158:29–43. https://doi.org/10.1016/j.quascirev.2016.12.021

Anzidei M, Bosman A, Carluccio R et al (2017) Flooding scenarios due to land subsidence and sea-level rise: a case study for Lipari Island (Italy). Terra Nova 29(1):44–51. https://doi.org/10.1111/ter.12246

Anzidei M, Scicchitano G, Tarascio S et al (2018) Coastal retreat and marine flooding scenario for 2100: a case study along the Coast of Maddalena Peninsula (southeastern Sicily). Geogr Fis Dinam, Quat 41:5–16. https://doi.org/10.4461/GFDQ.2018.41.9

Anzidei M, Doumaz F, Vecchio A (2020) Sea level rise scenario for 2100 A.D. In the heritage site of Pyrgi (Santa Severa, Italy). J Mar Sci Eng 8(2):64. https://doi.org/10.3390/jmse8020064

Anzidei M, Scicchitano G, Scardino G et al (2021) Relative Sea-Level rise scenario for 2100 along the coast of south eastern Sicily (Italy) by InSAR data, satellite images and high-resolution topography. Remote Sens 13(6):1108. https://doi.org/10.3390/rs13061108

Armaroli C, Duo E (2018) Validation of the coastal storm risk assessment framework along the Emilia-Romagna coast. Coast Eng 134:159–167. https://doi.org/10.1016/j.coastaleng.2017.08.014

Aucelli PPC, Di Paola G, Incontri P et al (2017) Coastal inundation risk assessment due to subsidence and sea level rise in a Mediterranean alluvial plain (Volturno coastal plain–southern Italy. Estuar Coastal Shelf Sci 198:597–609 https://doi.org/10.1016/j.ecss.2016.06.017

Aucelli PP, Di Paola G, Rizzo A et al (2018) Present day and future scenarios of coastal erosion and flooding processes along the Italian Adriatic coast: the case of Molise region. Environ Earth Sci 77:1–19 https://doi.org/10.1007/s12665-018-7535-y

Baldassini N, Di Stefano A (2017) Stratigraphic features of the Maltese Archipelago: a synthesis. Nat Hazards 86:203–231. https://doi.org/10.1007/s11069-016-2334-9

Batzakis D-V, Karymbalis E, Tsanakas K (2024) Assessing coastal vulnerability to climate change-induced hazards in the Eastern Mediterranean: A comparative review of methodological approaches. In: Petropoulos GP, Chalkias C (eds) Geographical Information Science. Elsevier, pp 253–278. https://doi.org/10.1016/B978-0-443-13605-4.00013-8

Beccari B (2016) A Comparative Analysis of Disaster Risk, Vulnerability and Resilience Composite Indicators. PLOS Curr Disasters. https://search.yahoo.com/search?ei=utf-8&fr=aaplw&p=10.1371/currents.dis.453df025e34b682e9737f95070f9b970.

Borzì L, Anfuso G, Manno G et al (2021) Shoreline evolution and environmental changes at the NW area of the Gulf of Gela (Sicily, Italy). Land 10(10):1034. https://doi.org/10.3390/land10101034

Brochier F, Ramieri E (2001) Climate change impacts on the mediterranean coastal zones. SSRN J. https://doi.org/10.2139/ssrn.277549

Bruno MF, Saponieri A, Molfetta MG et al (2020) The DPSIR approach for coastal risk assessment under climate change at regional scale: the case of Apulian Coast (Italy). J Mar Sci Eng 8(7):531. https://doi.org/10.3390/jmse8070531

Cappadonia C, Coratza P, Agnesi V et al (2018) Malta and Sicily joined by geoheritage enhancement and geotourism within the framework of land management and development. Geosciences 8(7):253. https://doi.org/10.3390/geosciences8070253

Castelli M, Torsello G, Vallero G (2021) Preliminary modeling of rockfall runout: definition of the input parameters for the QGIS plugin QPROTO. Geosciences 11(2):88. https://doi.org/10.3390/geosciences11020088

Christodoulou A, Christidis P, Demirel H (2019) Sea-level rise in ports: a wider focus on impacts. Marit Econ Logist 21:482–496. https://doi.org/10.1057/s41278-018-0114-z

Climate Change Post (2024) Available online: (accessed on 11th November 2025) https://www.climatechangepost.com/malta/coastal-floods/

Climate Data Store (2024) Retrieved January 18, 2024, from https://cds.climate.copernicus.eu/cdsapp#!/dataset/siswater-level-change-indicators?tab=overview

Coratza P, Bruschi VM, Piacentini D et al (2011) Recognition and assessment of geomorphosites in Malta at the Il-Majjistral Nature and History Park. Geoheritage 3:175–185. https://doi.org/10.1007/s12371-011-0034-0

Coratza P, Gauci R, Schembri J et al (2016) Bridging natural and cultural values of sites with outstanding scenery: evidence from Gozo, Maltese Islands. Geoheritage 8:91–103. https://doi.org/10.1007/s12371-015-0167-7

Corine Land Cover (2018) (vector/raster 100 m), Europe, 6-yearly. https://doi.org/10.2909/71c95a07-e296-44fc-b22b-415f42acfdf0

Cramer W, Guiot J, Fader M et al (2018) Climate change and interconnected risks to sustainable development in the Mediterranean. Nat Clim Change 8(11):972–980. https://doi.org/10.1038/s41558-018-0299-2

Da Lio C, Tosi L (2018) Land subsidence in the Friuli Venezia Giulia coastal plain, Italy: 1992–2010 results from SAR-based interferometry. Sci Total Environ 633:752–764. https://doi.org/10.1016/j.scitotenv.2018.03.244

Darwish K, Smith S (2023) Landsat-based assessment of morphological changes along the Sinai Mediterranean Coast between 1990 and 2020. Remote Sens 15(5):1392. https://doi.org/10.3390/rs15051392

Dasgupta S, Laplante B, Meisner C et al (2009) The impact of sea level rise on developing countries: a comparative analysis. Clim Change 93:379–388. https://doi.org/10.1007/s10584-008-9499-5

De Vivo C, Ellena M, Capozzi V et al (2022) Risk assessment framework for Mediterranean airports: a focus on extreme temperatures and precipitations and sea level rise. Nat Hazards 111:547–566. https://doi.org/10.1007/s11069-021-05066-0

Devoto S, Biolchi S, Bruschi VM et al (2012) Geomorphological map of the NW Coast of the Island of Malta (Mediterranean Sea). J Maps 8(1):33–40. https://doi.org/10.1080/17445647.2012.668425

Devoto S, Macovaz V, Mantovani M et al (2020) Advantages of using UAV digital photogrammetry in the study of slow-moving coastal landslides. Remote Sens 12(21):3566. https://doi.org/10.3390/rs12213566

Di Paola G, Rizzo A, Benassai G et al (2021) Sea-level rise impact and future scenarios of inundation risk along the coastal plains in Campania (Italy). Environ Earth Sci 80(17):608. https://doi.org/10.1007/s12665-021-09884-0

Dolan R, Fenster MS, Holme SJ (1991) Temporal analysis of shoreline recession and accretion. J Coastal Res 7(3):723–744

Enríquez AR, Marcos M, Falqués A et al (2019) Assessing beach and dune erosion and vulnerability under sea level rise: a case study in the Mediterranean Sea. Front Mar Sci 6:4. https://doi.org/10.3389/fmars.2019.00004

ERDF 156 Data (2013) Developing National environmental monitoring infrastructure and capacity. Malta Environment & Planning Authority, Malta

Farrugia MT (2008) Coastal erosion along northern Malta: geomorphological processes and risks. Geogr Fis Dinam Quat 31(2):149–160. https://www.gfdq.glaciologia.it/index.php/GFDQ/article/view/296

Ferreira O, Viavattene C, Jiménez JA et al (2018) Storm-induced risk assessment: evaluation of two tools at the regional and hotspot scale. Coast Eng 134:241–253. https://doi.org/10.1016/j.coastaleng.2017.10.005

Foglini F, Prampolini M, Micallef A et al (2016) Late Quaternary coastal landscape morphology and evolution of the Maltese Islands (Mediterranean Sea) reconstructed from high-resolution seafloor data. Geol Soc Lond Special Publications 4111:77–95. https://doi.org/10.1144/SP411.12

Formosa S (2015) Rising waters: Integrating national datasets for enhanced visualisation of diminishing spatial entities in a small Island state. Xjenza Online 3:105–117. https://doi.org/10.7423/XJENZA.2015.2.02

Frihy OE, El-Sayed MK (2013) Vulnerability risk assessment and adaptation to climate change induced sea level rise along the Mediterranean coast of Egypt. Mitig Adapt Strateg Glob Change 18:1215–1237. https://doi.org/10.1007/s11027-012-9418-y

Galea P (2019) Central mediterranean Tectonics—A key player in the geomorphology of the Maltese Islands. In: Gauci R, Schembri JA (eds) Landscapes and landforms of the Maltese Islands. Springer International Publishing, Cham, pp 19–30. https://doi.org/10.1007/978-3-030-15456-1_3

Gallina V, Torresan S, Critto A et al (2016) A review of multi-risk methodologies for natural hazards: consequences and challenges for a climate change impact assessment. J Environ Manage 168:123–132. https://doi.org/10.1016/j.jenvman.2015.11.011

Gallina V, Torresan S, Zabeo A et al (2020) A multi-risk methodology for the assessment of climate change impacts in coastal zones. Sustainability 12(9):3697. https://doi.org/10.3390/su12093697

Gauci R, Schembri JA (2019) Introduction to landscapes and landforms of the Maltese Islands. In: Gauci R, Schembri JA (eds) Landscapes and landforms of the Maltese Islands. Springer, Cham, pp 1–5. https://doi.org/10.1007/978-3-030-15456-1_1

Gauci R, Inkpen R, Soar PJ (2022) Spatial analysis of eroding surface micro-topographies. Mar Geol 452:106880. https://doi.org/10.1016/j.margeo.2022.106880

Geofabrik (2024) Available online: http://download.geofabrik.de/europe/malta.htm (accessed on 14 October

Giorgi F (2006) Climate change hot-spots. Geophys Res Lett 33(8):1–4. https://doi.org/10.1029/2006GL025734

Giorgi F, Lionello P (2008) Climate change projections for the Mediterranean region. Glob Planet Change 63(2–3):90–104. https://doi.org/10.1016/j.gloplacha.2007.09.005

Himmelstoss EA, Henderson RE, Farris AS et al (2024) Digital shoreline analysis system version 6.0: U.S. Geological Survey software release. https://doi.org/10.5066/P13WIZ8M

IPCC (1990) Climate Change: The IPCC Scientific Assessment. Houghton JT, Jenkins GJ, Ephraums JJ (eds). Cambridge University Press, Cambridge (Great Britain), New York (NY, USA) and Melbourne (Australia), pp 410. https://archive.ipcc.ch/publications_and_data/publications_ipcc_90_92_assessments_far.shtml

IPCC (2007) In: Metz B., Davidson OR, Bosch PR, Dave R, Meyer LA(eds) Climate change 2007: Mitigation. Contribution of working group III to the fourth assessment report of the intergovernmental panel on climate change.Cambridge University Press, Cambridge, United Kingdom and New York, NY, USA.

IPCC (2013) Summary for policymakers. In: Stocker TF, Qin D, Plattner G-K, Tignor M, Allen SK, Boschung J, Nauels A, Xia Y, Bex V, Midgley PM (eds) Climate change 2013: the physical science Basis. Contribution of working group I to the fifth assessment report of the intergovernmental panel on climate change . Cambridge University Press, Cambridge, United Kingdom and New York, NY, USA

IPCC (2023) Summary for policymakers. In: Core wrting team, Lee H, Romero J (eds) Climate change 2023: synthesis report. Contribution of working groups I, II and III to the sixth assessment report of the intergovernmental panel on climate change. IPCC, Geneva, Switzerland, pp 1–34. https://doi.org/10.59327/IPCC/AR6-9789291691647.001

Jaboyedoff M, Dudt JP, Labiouse V (2005) An attempt to refine rockfall hazard zoning based on the kinetic energy, frequency and fragmentation degree. Nat Hazards Earth Syst Sci 5(5):621–632. https://doi.org/10.5194/nhess-5-621-2005

Jiménez JA, Valdemoro HI, Bosom E et al (2017) Impacts of sea-level rise-induced erosion on the Catalan coast. Reg Environ Change 17:593–603. https://doi.org/10.1007/s10113-016-1052-x

Kefi C, Bakouche H, El Asmi AM (2024) Climate-induced vulnerability and conservation strategies for coastal heritage sites in the Southern Mediterranean Sea using integrated remote sensing and flood modeling. Reg Stud Mar Sci 77:103618. https://doi.org/10.1016/j.rsma.2024.103618

Khouakhi A, Snoussi M, Niazi S et al (2013) Vulnerability assessment of al Hoceima Bay (Moroccan Mediterranean coast): a coastal management tool to reduce potential impacts of sea-level rise and storm surges. J Coastal Res 65(10065):968–973. https://doi.org/10.2112/SI65-164.1

Kopp RE, Gilmore EA, Little CM et al (2019) Usable science for managing the risks of sea-level rise. Earth's Future 7(12):1235–1269. https://doi.org/10.1029/2018EF001145

Lambeck K, Antonioli F, Anzidei M et al (2011) Sea level change along the Italian coast during the Holocene and projections for the future. Quatern Int 232:250–257. https://doi.org/10.1016/j.quaint.2010.04.026

Lionello P, Scarascia L (2018) The relation between climate change in the Mediterranean region and global warming. Reg Environ Change 18:1481–1493. https://doi.org/10.1007/s10113-018-1290-1

Longobardi A, Boulariah O (2022) Long-term regional changes in inter-annual precipitation variability in the Campania Region, Southern Italy. Theor Appl Climatol 148(3):869–879. https://doi.org/10.1007/s00704-022-03972-2

Luijendijk A, Hagenaars G, Ranasinghe R et al (2018) The state of the world's beaches. Sci Rep 8:6641. https://doi.org/10.1038/s41598-018-24630-6

Lyra A, Loukas A, Sidiropoulos P, Mylopoulos N (2024) Climatic modeling of seawater intrusion in coastal aquifers: understanding the climate change impacts. Hydrology 11(4):49

Maanan M, Maanan M, Rueff H (2018) Assess the human and environmental vulnerability for coastal hazard by using a multi-criteria decision analysis. Hum Ecol Risk Assess Int J 24(6):1642–1658. https://doi.org/10.1080/10807039.2017.1421452

Main G, Schembri J, Gauci R et al (2018) The hazard exposure of the Maltese Islands. Nat Hazards 92:829–855. https://doi.org/10.1007/s11069-018-3227-x

Makris C, Tolika K, Baltikas V et al (2023) Climate change effects on the storm surges of the Mediterranean coastal zone. In: e-Proceedings of the 2nd International Scientific Conference on Design and Management of Port, Coastal and Offshore Works (DMPCO), Thessaloniki, Greece, 24–27 May 2023, pp 60–64

Manno G, Azzara G, Lo Re C et al (2023) An approach for the validation of a coastal erosion vulnerability index: an application in Sicily. J Mar Sci Eng 11(1):23. https://doi.org/10.3390/jmse11010023

Mantovani M, Devoto S, Forte E et al (2013) A multidisciplinary approach for rock spreading and block sliding investigation in the north-western coast of Malta. Landslides 10(5):611–622. https://doi.org/10.1007/s10346-012-0347-3

Mantovani M, Devoto S, Piacentini D et al (2016) Advanced SAR interferometric analysis to support geomorphological interpretation of slow-moving coastal landslides (Malta, Mediterranean Sea). Remote Sens 8(6):443. https://doi.org/10.3390/rs8060443

Marsico A, Lisco S, Lo Presti V et al (2017) Flooding scenario for four Italian coastal plains using three relative sea level rise models. J Maps 13(2):961–967. https://doi.org/10.1080/17445647.2017.1415989

Mayes J (2001) Rainfall variability in the Maltese Islands: changes, causes and consequences. Geography 86(2):121–130. https://doi.org/10.1080/20436564.2001.12219789

Mejjad N, Rossi A, Pavel AB (2022) The coastal tourism industry in the Mediterranean: a critical review of the socio-economic and environmental pressures & impacts. Tourism Manage Perspect 44:101007. https://doi.org/10.1016/j.tmp.2022.101007

Mel RA, Coraci E, Morucci S et al (2023) Insights on the extreme storm surge event of the 22 November 2022 in the Venice Lagoon. J Mar Sci Eng 11(9):1750. https://doi.org/10.3390/jmse11091750

Menna M, Gačić M, Martellucci R et al (2022) Climatic, decadal, and interannual variability in the upper layer of the Mediterranean Sea using remotely sensed and in-situ data. Remote Sens 14(6):1322. https://doi.org/10.3390/rs14061322

Micallef A, Foglini F, Le Bas T et al (2013) The submerged paleolandscape of the Maltese Islands: morphology, evolution and relation to Quaternary environmental change. Mar Geol 335:129–147 https://doi.org/10.1016/j.margeo.2012.10.017

Micallef S, Micallef A, Galdies C (2018) Application of the Coastal Hazard Wheel to assess erosion on the Maltese coast. Ocean Coastal Manage 156:209–222. https://doi.org/10.1016/j.ocecoaman.2017.06.005

Mifsud Scicluna B, Galdies C (2025) Assessing the impact of temperature and precipitation trends of climate change on agriculture based on multiple global circulation model projections in Malta. Big Data Cogn Comput 9(4):105. https://doi.org/10.3390/bdcc9040105

Molina R, Manno G, Lo Re C, Anfuso G, Ciraolo G (2020) A methodological approach to determine sound response modalities to coastal erosion processes in Mediterranean Andalusia (Spain). J Mar Sci Eng 8(3):154. https://doi.org/10.3390/jmse8030154

Monioudi IN, Velegrakis AF, Chatzipavlis AE et al (2017) Assessment of island beach erosion due to sea level rise: the case of the Aegean archipelago (Eastern Mediterranean). Nat Hazards Earth Syst Sci 17:449–466. https://doi.org/10.5194/nhess-17-449-2017

Nicholls RJ, Cazenave A (2010) Sea-level rise and its impact on coastal zones. Science 328(5985):1517–1520. https://doi.org/10.1126/science.1185782

Nicholls RJ, Hoozemans FMJ (1996) The mediterranean: vulnerability to coastal implications of climate change. Ocean Coastal Manage 31(2–3):105–132. https://doi.org/10.1016/S0964-5691(96)00037-3

NSO - National Statistics Office (2019) Social protection—Reference Years 2012–2016. Malta, 2019. Available online: https://nso.gov.mt/en/publicatons/Publications_by_Unit/Documents/A2_Public_Finance/Social%20Protection%202016.pdf. Accessed on 8 Oct 2024

NSO - National Statistics Office (2022) The state of the climate 2022: A multidecadal report and assessment of Malta's climate (reference year 2020). National Statistics Office, Valletta, Malta.Retrieved from https://nso.gov.mt/wp-content/uploads/Climate-publication-2022.pdf

Oyedotun TDT (2014) Sect. 3.2.2: Shoreline geometry: DSAS as a tool for historical trend analysis. In: Clarke LE, Nield JM (eds) Geomorphological techniques (Online Edition). British Society for Geomorphology, London, UK

Pantusa D, D'Alessandro F, Frega F et al (2022) Improvement of a coastal vulnerability index and its application along the Calabria Coastline, Italy. Sci Rep 12(1):21959. https://doi.org/10.1038/s41598-022-26374-w

Pappone G, Aucelli PPC, Aberico I et al (2012) Relative sea-level rise and marine erosion and inundation in the Sele river coastal plain (Southern Italy): scenarios for the next century. Rend Fis Acc Lincei 23:121–129

Pedley HM, House MR, Waugh B (1978) The geology of the pelagian block: the Maltese Islands. In: Nairn AEM, Kanes WH, Stehli FG (eds) The ocean basins and margins. Springer US, Boston, MA, pp 417–433. https://doi.org/10.1007/978-1-4684-3039-4_8

Perini L, Calabrese L, Luciani P et al (2017) Sea-level rise along the Emilia-Romagna coast (Northern Italy) in 2100: scenarios and impacts. Nat Hazards Earth Syst Sci 17(12):2271–2287. https://doi.org/10.5194/nhess-17-2271-2017

Possenelli M, Gauci R, Devoto S et al (2024) Inventory and quantitative assessment of geosites in the southern sector of the Island of Malta. Geosciences 14(11):292. https://doi.org/10.3390/geosciences14110292

Prampolini M, Foglini F, Biolchi S et al (2017) Geomorphological mapping of terrestrial and marine areas, northern Malta and Comino (central Mediterranean Sea). J Maps 13(2):457–469. https://doi.org/10.1080/17445647.2017.1327507

Prampolini M, Foglini F, Micallef A et al (2019) Malta's submerged landscapes and landforms. In: Gauci R, Schembri JA (eds) Landscapes and landforms of the Maltese Islands. Springer, Switzerland, pp 117–128. https://doi.org/10.1007/978-3-030-15456-1_10

Prampolini M, Savini A, Foglini F et al (2020) Seven good reasons for integrating terrestrial and marine spatial datasets in changing environments. Water 12(8):2221. https://doi.org/10.3390/w12082221

Reimann L, Vafeidis AT, Brown S (2018) Mediterranean UNESCO world heritage at risk from coastal flooding and erosion due to sea-level rise. Nat Commun 9(1):4161. https://doi.org/10.1038/s41467-018-06645-9

Rizzo A, Aucelli PPC, Gracia FJ et al (2018) A novelty coastal susceptibility assessment method: application to Valdelagrana area (SW Spain). J Coast Conserv 22:973–987. https://doi.org/10.1007/s11852-017-0552-2

Rizzo A, Vandelli V, Buhagiar G et al (2020) Coastal vulnerability assessment along the north-eastern sector of Gozo Island (Malta, Mediterranean Sea). Water 12(5):1405. https://doi.org/10.3390/w12051405

Rizzo A, Vandelli V, Gauci C et al (2022) Potential sea level rise inundation in the Mediterranean: from susceptibility assessment to risk scenarios for policy action. Water 14(3):416. https://doi.org/10.3390/w14030416

Rizzo A, Mattei G, Steenssens LD et al (2025) Methodological advances in sea level rise vulnerability assessment: implications for sustainable coastal management in a climate change scenario. Ocean Coastal Manage 268:107751

Rossi S, Vandelli V, Bucci MG et al (2024) Geoscience studies in the Maltese Islands: a gateway to the Central Mediterranean region. Ital J Geosci 143(2):299–313. https://doi.org/10.3301/IJG.2024.15

Rossi S, Keimeris D, Papachristou C et al (2025a) Preliminary assessment of long-term sea-level rise-induced inundation in the deltaic system of the northern coast of the Amvrakikos Gulf (Western Greece). J Mar Sci Eng 13:2114. https://doi.org/10.3390/jmse13112114

Rossi S, Prampolini M, Galea C et al (2025b) Geomorphological evidence of the Malta-Sicily land-bridge during the Last Glacial Maximum inferred from seismic profiles. Earth Surf Proc Land 50(2):e6061. https://doi.org/10.1002/esp.6061

Russo B, Paindelli A, Yubero Pena D, Locatelli L (2022) Use of social media crowdsourcing data for pluvial flood modelling validation to assess future climate-related impacts: The CRISI ADAPT Project. In M. Ortega-Sánchez (Ed.), Proceedings of the 39th IAHR World Congress (Granada, 2022). International Association for Hydro-Environment Engineering and Research, pp 7110–7120 https://doi.org/10.3850/IAHR-39WC2521716X20221669

Salman A, Lombardo S, Doody P (2004) Living with Coastal Erosion in Europe: Sediment and Space for Sustainability; Technical Report; EUCC: Warnemünde, Germany

Santos D, Abreu T, Bernardes C et al (2024) Coastal flood susceptibility assessment along the Northern coast of Portugal. Int J Disaster Risk Reduct 108:104556 https://doi.org/10.1016/j.ijdrr.2024.104556

Sarkar N, Rizzo A, Vandelli V et al (2022) A literature review of climate-Related coastal risks in the Mediterranean, a climate change hotspot. Sustainability 14(23):15994. https://doi.org/10.3390/su142315994

Sarkar N, Devoto S, Vandelli V et al (2024) Rock-fall runout simulation using a QGIS plugin along north–west coast of Malta (Mediterranean Sea). Nat Hazards. https://doi.org/10.1007/s11069-024-06821-9

Scardino G, Sabatier F, Scicchitano G et al (2020) Sea-level rise and shoreline changes along an open sandy coast: case study of Gulf of Taranto, Italy. Water 12(5):1414 https://doi.org/10.3390/w12051414

Scardino G, Anzidei M, Petio P et al (2022) The impact of future sea-level rise on low-lying subsiding coasts: a case study of Tavoliere delle Puglie (Southern Italy). Remote Sens 14(19):4936. https://doi.org/10.3390/rs14194936

Scavia C, Barbero M, Castelli M et al (2020) Evaluating rockfall risk: some critical aspects. Geosciences 10(3):98. https://doi.org/10.3390/geosciences10030098

Scerri S (2019) Sedimentary evolution and resultant geological landscapes. In: Gauci R, Schembri JA (eds) Landscapes and landforms of the Maltese Islands. Springer, Cham, pp 31–47. https://doi.org/10.1007/978-3-030-15456-1_4

Schembri JA (2019) The geographical context of the Maltese Islands. In: Gauci R, Schembri JA (eds) Landscapes and landforms of the Maltese Islands. Springer, Berlin, Cham, pp 9–17 https://doi.org/10.1007/978-3-030-15456-1_2

Schuerch M, Kiesel J, Boutron O et al (2025) Large-scale loss of Mediterranean coastal marshes under rising sea levels by 2100. Commun Earth Environ 6(1):128 https://doi.org/10.1038/s43247-025-02099-2

Scott D, Hall CM, Gössling S (2019) Global tourism vulnerability to climate change. Annals Tourism Res 77:49–61. https://doi.org/10.1016/j.annals.2019.05.007

Selmi L, Coratza P, Gauci R et al (2019) Geoheritage as a tool for environmental management: a case study in northern Malta (Central Mediterranean Sea). Resources 8(4):168. https://doi.org/10.3390/resources8040168

Serpelloni E, Vannucci G, Pondrelli S et al (2007) Kinematics of the Western Africa-Eurasia plate boundary from focal mechanisms and GPS data. Geophys J Int 169(3):1180–1200. https://doi.org/10.1111/j.1365-246X.2007.03367.x

Serpelloni E, Faccenna C, Spada G et al (2013) Vertical GPS ground motion rates in the Euro-Mediterranean region: new evidence of velocity gradients at different spatial scales along the Nubia-Eurasia plate boundary. J Geophys Res: Solid Earth 118(11):6003–6024. https://doi.org/10.1002/2013JB010102

Soldati M, Barrows TT, Prampolini M et al (2018) Cosmogenic exposure dating constraints for coastal landslide evolution on the Island of Malta (Mediterranean Sea). J Coast Conserv 22:831–844. https://doi.org/10.1007/s11852-017-0551-3

Soldati M, Devoto S, Prampolini M et al (2019) The spectacular landslide-controlled landscape of the northwestern coast of Malta. In: Gauci R, Schembri JA (eds) Landscapes and landforms of the Maltese Islands. Springer, Cham, pp 167–178. https://doi.org/10.1007/978-3-030-15456-1_14

Spiteri L, Stevens DT (2019) Landscape diversity and protection in Malta. In: Gauci R, Schembri JA (eds) Landscapes and landforms of the Maltese Islands. Springer International Publishing, Cham, pp 359–372. https://doi.org/10.1007/978-3-030-15456-1_28

Tarragoni C, Bellotti P, Davoli L et al (2014) Assessment of coastal vulnerability to erosion: the case of Tiber River delta (Tyrrhenian Sea, central Italy). Italian J Eng Geol Environ 2:5–16. https://doi.org/10.4408/IJEGE.2014-02.O-01

Thiéblemont R, Le Cozannet G, Rohmer J et al (2024) Sea-level rise induced change in exposure of low-lying coastal land: implications for coastal conservation strategies. Anthropocene Coasts 7(1):8

Thieler ER, Himmelstoss EA, Zichichi JL et al (2009) The Digital Shoreline Analysis System (DSAS) Version 4.0—An ArcGIS extension for calculating shoreline change. Open-File Report. https://doi.org/10.3133/ofr20081278

Todaro V, D'Oria M, Secci D et al (2022) Climate change over the Mediterranean region: local temperature and precipitation variations at five pilot sites. Water 14(16):2499. https://doi.org/10.3390/w14162499

Torresan S, Critto A, Rizzi J et al (2012) Assessment of coastal vulnerability to climate change hazards at the regional scale: the case study of the North Adriatic Sea. Nat Hazards Earth Syst Sci 12(7):2347–2368. https://doi.org/10.5194/nhess-12-2347-2012

Tosi L, Carbognin L, Teatini P et al (2002) Evidence of the present relative land stability of Venice, Italy, from land, sea, and space observations. Geophys Res Lett 29(12):3–1. https://doi.org/10.1029/2001GL013211

Tosi L, Da Lio C, Strozzi T et al (2016) Combining L-and X-band SAR interferometry to assess ground displacements in heterogeneous coastal environments: the Po River Delta and Venice Lagoon, Italy. Remote Sens 8(4):308. https://doi.org/10.3390/rs8040308

Tursi MF, Anfuso G, Matano F et al (2023) A methodological tool to assess erosion susceptibility of high coastal sectors: case studies from Campania region (Southern Italy). Water 15:121. https://doi.org/10.3390/w15010121

Tursi MF, Anfuso G, Manno G et al (2025) A multi component approach to predict erosion susceptibility of rocky coasts: marine, terrestrial and climatic forcing—An application in Southern Italy. Environ Earth Sci 84(7):183. https://doi.org/10.1007/s12665-025-12143-1

Vandelli V, Sarkar N, Micallef AS et al (2023) Coastal inundation scenarios in the north-eastern sector of the Island of Gozo (Malta, Mediterranean Sea) as a response to sea level rise. J Maps 19(1):2145918. https://doi.org/10.1080/17445647.2022.2145918

Velegrakis AF, Monioudi IN, Vousdoukas MI et al (2023) Drivers and impacts of beach erosion in Eastern Mediterranean Islands. In: 18th International Conference on Environmental Science and Technology, Athens, Greece

Zammit Pace ML, Bray M, Potts J et al (2019) The beaches of the Maltese Islands: A valuable but threatened resource? In: Gauci R, Schembri JA (eds) Landscapes and landforms of the Maltese Islands. Springer, Cham, pp 213–227 https://doi.org/10.1007/978-3-030-15456-1_18

Publisher's note Springer Nature remains neutral with regard to jurisdictional claims in published maps and institutional affiliations.

Springer Nature or its licensor (e.g. a society or other partner) holds exclusive rights to this article under a publishing agreement with the author(s) or other rightsholder(s); author self-archiving of the accepted manuscript version of this article is solely governed by the terms of such publishing agreement and applicable law.

Authors and Affiliations

Nabanita Sarkar[1,2] · Angela Rizzo[3,4] · Vittoria Vandelli[5] · Mauro Soldati[5]

✉ Vittoria Vandelli
vittoria.vandelli@unimore.it

Nabanita Sarkar
nabanita.sarkar@iusspavia.it

Angela Rizzo
angela.rizzo@uniba.it

Mauro Soldati
mauro.soldati@unimore.it

[1] Institute of Marine Sciences (ISMAR-CNR), 40129 Bologna, Italy

[2] School for Advanced Studies (IUSS) of Pavia, 27100, Pavia, Italy

[3] Interdepartmental Research Center for Coastal Dynamics, University of Bari Aldo Moro, 70125 Bari, Italy

[4] Department of Earth and Geo-Environmental Sciences, University of Bari Aldo Moro, 70125 Bari, Italy

[5] Department of Chemical and Geological Sciences, University of Modena and Reggio Emilia, 41125 Modena, Italy